

University of Windsor

Scholarship at UWindor

Electronic Theses and Dissertations

Theses, Dissertations, and Major Papers

1-1-1966

An experimental investigation of the effects of an initial gap on the jet flow over a curved wall.

Suresh C. Paranjpe
University of Windsor

Follow this and additional works at: <https://scholar.uwindsor.ca/etd>

Recommended Citation

Paranjpe, Suresh C., "An experimental investigation of the effects of an initial gap on the jet flow over a curved wall." (1966). *Electronic Theses and Dissertations*. 6444.
<https://scholar.uwindsor.ca/etd/6444>

This online database contains the full-text of PhD dissertations and Masters' theses of University of Windsor students from 1954 forward. These documents are made available for personal study and research purposes only, in accordance with the Canadian Copyright Act and the Creative Commons license—CC BY-NC-ND (Attribution, Non-Commercial, No Derivative Works). Under this license, works must always be attributed to the copyright holder (original author), cannot be used for any commercial purposes, and may not be altered. Any other use would require the permission of the copyright holder. Students may inquire about withdrawing their dissertation and/or thesis from this database. For additional inquiries, please contact the repository administrator via email (scholarship@uwindsor.ca) or by telephone at 519-253-3000ext. 3208.

AN EXPERIMENTAL INVESTIGATION OF
THE EFFECTS OF AN INITIAL GAP
ON THE JET FLOW OVER A CURVED WALL

A THESIS

Submitted to the Faculty of Graduate
Studies through the Department of
Mechanical Engineering in Partial
Fulfilment of the requirements for
the Degree of Master of Applied
Science at the University of Windsor.

By

SURESH C. PARANJPE

B.Sc. (Engg.), The Birla Institute of Tech.

Ranchi, India, 1962.

Windsor, Ontario, Canada.

1966

UMI Number: EC52625

INFORMATION TO USERS

The quality of this reproduction is dependent upon the quality of the copy submitted. Broken or indistinct print, colored or poor quality illustrations and photographs, print bleed-through, substandard margins, and improper alignment can adversely affect reproduction.

In the unlikely event that the author did not send a complete manuscript and there are missing pages, these will be noted. Also, if unauthorized copyright material had to be removed, a note will indicate the deletion.

UMI[®]

UMI Microform EC52625

Copyright 2008 by ProQuest LLC.

All rights reserved. This microform edition is protected against unauthorized copying under Title 17, United States Code.

ProQuest LLC
789 E. Eisenhower Parkway
PO Box 1346
Ann Arbor, MI 48106-1346

PLX 6214

Approved By:

St. L. E. ...

D. E. L. Maclean

Henry J. Tucker

134567

ABSTRACT

The flow in a two dimensional curved wall jet with different initial gaps between the nozzle exit and the leading edge of the wall was probed at various stations along the jet. The jet slot thickness, jet exit velocity, and radius of the wall were kept constant. It was found that the region close to the leading edge of the wall behaved like a settling zone. In this zone, the type of flow changed from free jet to a curved wall jet. The length required for settling depended on gap size and was less than that of the plane wall jet. Gap effects on surface pressure distribution and angular position of separation were examined. The hysteresis phenomenon associated with gaps was investigated.

ACKNOWLEDGEMENTS

The author is indebted to Prof. W.G. Colborne for providing the opportunity to pursue this investigation and for his continued support and encouragement.

The author would like to express his gratitude to Dr. K. Sridhar for his supervision, generous guidance and help throughout this work.

Thanks are due to Professor H.J. Tucker for his helpful advice. The technical assistance of Mr. O. Brudy in constructing the apparatus is very much appreciated.

The research for this thesis was supported by the Defence Research Board of Canada, Grant number 9550-20 and the National Research Council of Canada, Grant number A-2190.

TABLE OF CONTENTS

ABSTRACT	Page ii
NOTATION	v.i
LIST OF FIGURES	ix
I INTRODUCTION	1
II LITERATURE SURVEY	3
2.1 NON-VISCOUS THEORY	3
2.2 REMARKS ON REAL JET FLOW	4
2.3 NEWMAN'S ANALYSIS	4
2.3.1. DIMENSIONAL APPROACH	4
2.3.2. THEORETICAL TREATMENT	6
2.4 NAKAGUCHI'S METHOD	8
2.5 GAP EFFECT	11
III TEST FACILITIES	13
3.1 AIR SUPPLY AND GUIDING DUCT	13
3.2 CONTRACTION DUCT AND NOZZLE	13
3.3 WALL AND TRAVERSING MECHANISM	14
3.4 PROBING EQUIPMENT	14
IV EXPERIMENTS	15
4.1 CALIBRATION	16
4.2 HYSTERESIS	17
4.3 WALL PRESSURE MEASUREMENTS	17
4.4 MEASUREMENT OF JET VELOCITY	18
4.5 VISUALIZATION OF FLOW SEPARATION	19
V EXPERIMENTAL RESULTS	20

5.1	DATA REDUCTION	Page 20
5.2	PRESENTATION AND DISCUSSION OF RESULTS	20
5.2.1.	HYSTERESIS	20
5.2.2.	VELOCITY PROFILES	21
5.2.3.	JET GROWTH	23
5.2.4.	MAXIMUM VELOCITY DECAY	25
5.2.5.	SURFACE PRESSURE DISTRIBUTION	25
5.2.6.	SEPARATION	26
VI	CONCLUSIONS	28
6.1.	CURVED WALL JET WITHOUT A GAP	28
6.2	CURVED WALL JET WITH A GAP	28
	REFERENCES	30
	FIGURES	31 to 59
	TABLE I	60
	VITA AUCTORIS	61

NOTATION

b	Distance between nozzle lip and leading edge of deflection surface, perpendicular to the axis of the nozzle (ft.). See Fig. 1.
b'	Non-dimensional b $(b' = \frac{b}{t})$.
Cp	Pressure coefficient = $\frac{(P_a - P_s) R_o}{(P_T - P_a) t}$.
l	Distance between nozzle lip and leading edge of deflection surface, parallel to the axis of the nozzle (ft.). See Fig. 1.
l'	Non-dimensional $(l' = \frac{l}{t})$.
m'	Difference between the b' values of "attached" and "detached" positions for a given .
n	Constant in Eqn. 2.12.
p	Static pressure (lbs./ft. ²).
P _a	Atmospheric pressure (lbs./ft. ²).
P _s	Static pressure on the wall (lbs./ft. ²).
P _T	Total pressure in the jet at the nozzle exit (lbs./ft. ²).
Re	Reynold's number = $\frac{(P_T - P_a) R_o t}{2} \frac{1}{2}$.
R _o	Radius of the wall (ft.).

s	Distance measured along deflection surface from its leading edge (ft.).
s'	Non-dimensional s ($s' = \frac{s}{t}$)
t	Jet slot thickness (ft.).
u	Mean velocity parallel to the jet axis (ft./sec.).
U _m	Maximum value of u at a given station (ft./sec.).
U ₀	Mean velocity of jet at the slot (ft./sec.).
u'	Tangential component of velocity fluctuation (ft./sec.).
v'	Radial component of velocity fluctuation (ft./sec.).
y	Distance from and normal to the wall of the wall jet or normal to the centre line of the free jet (ft./sec.). See Fig. 2.
Y _m	Value of y for which u is maximum (ft./sec.).
Y _m /2	Larger value of y for which u = 1/2 u _m (ft./sec.).
∞	Disposable constant in Glauert's theory (Ref. 1).
ε	Eddy viscosity (Slugs/ft.sec.).
θ	Angular position measured from the leading edge (degrees).

θ_{sep} Angular position of separation.

ν Kinematic viscosity (ft^2/sec).

ρ Density of the fluid (slugs/ft^3).

LIST OF FIGURES

	Page
Fig. 1 SCHEMATIC DIAGRAM OF TEST FACILITIES	31
Fig. 2 CURVED WALL JET NOMENCLATURE	32
Fig. 3 STATIC AND TOTAL PRESSURE PROBES	33
Fig. 4 FLOW PICTURE FOR NON-VISCOUS THEORY	33
Fig. 5 VIEW OF EXPERIMENTAL ARRANGEMENT	34
Fig. 6 STATIC PRESSURE PROBE CALIBRATION	35
Fig. 7 TWO DIMENSIONALITY CHECK	36
Fig. 8 HYSTERESIS PLOTS	37
Fig. 9 LEADING EDGE POSITIONS ALONG THE JET BOUNDARY	38
Fig.10 VISUALIZATION OF FLOW SEPARATION	39
Fig.11 SKETCH OF LAMP BLACK TRACES ON CURVED SURFACE	40
Fig.12 NON-DIMENSIONAL VELOCITY PROFILE OF CURVED WALL JET WITHOUT A GAP	41
Fig.13 NON-DIMENSIONAL VELOCITY PROFILE OF CURVED WALL JET WITH GAPS ALONG JET BOUNDARY	42 to 45
Fig.14 NON-DIMENSIONAL VELOCITY DISTRIBUTION IN THE OUTER LAYER	46
Fig.15 DIMENSIONAL VELOCITY PROFILES AT $\theta = 30^\circ$ FOR THE GAPS ALONG THE JET BOUNDARY	47
Fig.16 STATIC PRESSURE DISTRIBUTIONS IN THE JET FOR NO GAP	48
Fig.17 GROWTH OF CURVED WALL JET FOR GAPS ALONG JET BOUNDARY	49
Fig.18 OUTER LAYER GROWTH FOR GAPS ALONG JET BOUNDARY	50
Fig.19 INNER LAYER GROWTH FOR GAPS ALONG JET BOUNDARY	51

Fig. 20	STREAMWISE VARIATION OF $\frac{Y_m/2}{Ro\theta}$ WITH $\frac{Y_m/2}{Ro}$ FOR THE GAPS ON JET BOUNDARY	52
Fig. 21	MAXIMUM VELOCITY DECAY OF CURVED WALL JET WITH GAPS ALONG JET BOUNDARY	53
Fig. 22	MAXIMUM VELOCITY DECAY PLOTS (NEWMAN'S METHOD)	54
Fig. 23	SURFACE PRESSURE DISTRIBUTIONS	55 to 57
Fig. 24	ANGLE OF SEPARATION FOR THE GAPS ALONG THE JET BOUNDARY AND "ATTACHED" LINE	58
Fig. 25	PLOTS OF $\theta_{sep.}$ VS b' FOR DIFFERENT l'	59

CHAPTER I

INTRODUCTION

The phenomenon of a jet emerging tangentially to a curved wall and flowing along the surface of the wall has long been known as the "Coanda Effect." Recently many applications have been found for this phenomenon such as: blown flaps and jet flaps for high lift devices, and improvement of the efficiency of an internal flow system.

Because of the dominating turbulent mixing in the major outer part of the flow as well as considerable viscous effect in a part near the wall surface, the nature of the flow is evidently complex. Newman (Ref. 2), Nakaguchi (Ref. 3), Sawyer (Ref. 4), Fekete (Ref. 5) have done considerable work in this field. But in all these investigations, no gap was introduced between the curved surface and the nozzle exit.

Obviously, deflection surfaces with initial gaps are preferable for practical applications. Korbacher (Ref. 6) and Benner (Ref. 8) investigated the gap effect by measuring the force acting on and the surface pressure distribution over a quadrant surface. They did no flow measurement in the jet. The present investigation proposes to find the effect of a gap on the well established

velocity profiles, position of separation, static pressure distribution and to study the hysteresis phenomenon associated with gaps. The surrounding fluid was stationary and flow was in the incompressible range.

CHAPTER II

LITERATURE SURVEY

The material covered in this chapter summarizes briefly the existing literature and is included in the report for the sake of completeness and ease of reference. The present investigation requires a knowledge of the jet flow over a curved wall without an initial gap to find the effect of the gap. The investigations of the jet flow over a curved wall without a gap are considered in the following sections.

2.1 NON-VISCOUS THEORY

The bending of a jet sheet with one free and one bound surface is produced by a pressure difference acting across it. Consider an element (see Fig. 4) in a two dimensional flow of a thin jet ($t \ll R_0$). Assume that the velocity and thickness of the jet remain constant. Acting on the flow element are the centrifugal and the pressure forces which are in radial equilibrium. Therefore,

$$\rho \cdot R_0 \cdot d\theta \cdot t \cdot \frac{U_0^2}{R_0} = R_0 \cdot d\theta \cdot (P_a - P_s)$$

$$\therefore (P_a - P_s) = \rho \frac{t}{R_0} U_0^2$$

But from Bernoulli's equation,

$$\frac{1}{2} \rho U_0^2 = (P_T - P_a)$$

The pressure coefficient, C_p becomes

$$C_p = \frac{(P_a - P_s)}{(P_T - P_a)} \cdot \frac{R_0}{t} = 2 \quad (2.1)$$

Experimental results of Korbacher (Ref. 6) for small values of θ agree well with the above equation. But the values obtained by Newman (Ref. 2) and Fekete (Ref. 5) are less than that predicted by the above theory.

2.2 REMARKS ON REAL JET FLOW

The real fluid jet continuously entrains fluid from the surroundings. Thus the jet width increases and the fluid velocity decreases with increasing θ . In consequence, the pressure at the surface which is initially lower than P_a due to the flow curvature, tends to approach P_a as the jet velocity decreases. Hence the entrainment of the surrounding fluid produces the pressure rise that finally causes the boundary layer to separate from the surface. This emphasises the necessity of including the process of entrainment in any theoretical analysis.

2.3 NEWMAN'S ANALYSIS

2.3.1 DIMENSIONAL APPROACH

The following parameters are sufficient to define an incompressible jet flow over a curved surface:

$$(P_T - P_a), t, R_0, \gamma \text{ and } \theta.$$

The pressure difference across the jet sheet ($P_a - P_s$)

at angular position θ , may therefore be related non-dimensionally to these parameters as follows:

$$\frac{(P_a - P_s)}{(P_T - P_a)} = f \left[\theta, \frac{t}{R_o}, \left\{ \frac{(P_T - P_a) R_o^2}{\rho \nu^2} \right\}^{\frac{1}{2}} \right] \quad (2.2)$$

At some distance from the slot we might expect the flow to become independent of the separate parameters $(P_T - P_a)$ and t and depend only on their product $(P_T - P_a) \cdot t$ as long as suitable zero is chosen for θ . Furthermore for large values of Reynolds number the flow will tend to become independent of viscosity so that

$$\frac{(P_a - P_s) R_o}{(P_T - P_a) t} = f(\theta) \quad (2.3)$$

Similar results can be stated for the angular position of separation θ_{sep} . as follows:

$$\theta_{sep} = f \left[\frac{t}{R_o}, \left\{ \frac{(P_T - P_a) R_o t}{\rho \nu^2} \right\}^{\frac{1}{2}} \right] \quad (2.4)$$

If the position of separation is sufficiently far from the slot, then θ_{sep} . will depend only on Re .

$$\theta_{sep} = f \left[\left\{ \frac{(P_T - P_a) R_o t}{\rho \nu^2} \right\}^{\frac{1}{2}} \right] \quad (2.5)$$

At large Reynolds number θ_{sep} . with suitably chosen zero, tends to become constant. In particular, for small values of $\frac{t}{R_o}$, θ_{sep} . measured from the slot is constant. Experimental results (Ref. 2) confirm the above statement and they show that for $\frac{t}{R_o}$ values ranging from 0.02 to 0.4, $\theta_{sep} = 240^\circ$.

2.3.2 THEORETICAL TREATMENT

Information from the plane wall jet flow was used by Newman (Ref. 2) to get an approximate picture of the jet flow over a curved wall. For plane wall jets the skin friction can be considered negligible compared to the jet momentum at sufficiently high Re . Hence, jet momentum is practically conserved. Further, the flows having the same jet momentum, but which emerge from the slots having various widths, produce the same velocity profiles far downstream provided a suitable origin is chosen for the streamwise co-ordinate.

Newman therefore assumed that for the curved flow the skin friction was also small compared to the jet momentum at high Reynolds number. Hence the sum of the moment of momentum and the moment of pressure forces about the centre of the circular cylinder is constant. In applying this concept, it was assumed that streamlines are circles with the same centre as the cylindrical wall. Further, the velocity profiles are assumed to be similar at all downstream positions and that they can be replaced by a uniform velocity profile having the same mass flow and the same momentum. On the basis of these assumptions, Newman developed the expressions for the surface pressure distribution, the decay of the maximum velocity and the jet growth.

The relationship for the static pressure on the wall is

$$\frac{(P_a - P_s) R_0}{(P_T - P_a) \cdot t} = \frac{8 \ln \left(1 + \frac{4}{3} \frac{y_{m/2}}{R_0} \right)}{\left[\left(\frac{4}{3} \frac{y_{m/2}}{R_0} + 1 \right)^2 - 1 + 2 \ln \left(1 + \frac{4}{3} \frac{y_{m/2}}{R_0} \right) \right]} \quad (2.6)$$

Though the theory correctly predicts an adverse pressure gradient at the surface, the actual level of pressure is about 30 per cent too low. This is, as explained by Fekete (Ref. 5), due to the effect of the slot boundary layers on jet momentum.

The ratio of the actual to theoretical momentum, K , is always less than one. For Fekete's experiments, the value of K is 0.75. The surface pressure coefficient is corrected as follows to account for the boundary layers in the slot

$$C_p = \frac{(P_a - P_s) R_0}{(P_T - P_a) t K} \quad (2.7)$$

The correction gives a fairly good agreement between the theory and experiment.

Newman showed that the growth of the jet can be expressed as

$$\frac{y_{m/2}}{R_0 (\theta + c_1 \cdot t/R_0)} = C \left(1 + k \frac{y_{m/2}}{R_0} \right) \quad (2.8a)$$

Where $C_1 \cdot \frac{t}{R_0}$ is the correction for hypothetical origin.

For small $\frac{t}{R_0}$, the equation becomes

$$\frac{y_{m/2}}{R_0 \theta} = C \left(1 + k \frac{y_{m/2}}{R_0} \right) \quad (2.8b)$$

Downstream distance is replaced by $(R_0 + k y_{m/2}) \cdot \theta$ where k is an experimental constant of the order of unity. C is a constant for a given value of eddy viscosity. For a wall jet, $C = 0.085$ when $\frac{y_m}{y_{m/2}} = 0.14$ decreasing to $C = 0.073$ when $\frac{y_m}{y_{m/2}} = 0$ (i.e. infinite Re). For a free

jet $C = 0.114$. For curved jet, Newman found the relation experimentally as

$$\frac{y_{m/2}}{R_0 \theta} = 0.11 \left(1 + 1.5 \frac{y_{m/2}}{R_0} \right) \quad (2.9)$$

Table I gives constants obtained by other investigators.

The jet width therefore, increases more rapidly than a plane wall jet and for $\frac{y}{y_{m/2}} > 0.05$, the effective eddy viscosity is similar to that of a free jet. This is attributed to an increased mixing associated with the flow curvature in the outer part of the flow where $u_x (y + R_0)$ decreases with y .

Reduction of maximum jet velocity u_m around the cylinder at high Re is given by

$$\frac{\rho u_m^2 R_0 \theta}{(P_T - P_a) t} = \frac{128}{9} \theta \left[\left(\frac{4}{3} \frac{y_{m/2}}{R_0} + 1 \right)^2 - 1 + 2 \ln \left(1 + \frac{4}{3} \frac{y_{m/2}}{R_0} \right) \right]^{-1} \quad (2.10)$$

Where $\frac{y_{m/2}}{R_0}$ is related to θ by Equation (2.9). Agreement between the measured and theoretical values of $\frac{\rho u_m^2 R_0 \theta}{(P_T - P_a) t}$ is satisfactory.

Experimental results of Newman (Ref. 2) and Fekete (Ref. 5) show that the velocity profiles are similar over the major portion of the flow except near separation, and are in good agreement with Glauert's plane wall jet theory for $\frac{y_m}{y_{m/2}} = 0.14$.

2.4 NAKAGUCHI'S METHOD

Nakaguchi (Ref. 3) made a comprehensive theoretical analysis for incompressible flows by solving the Navier-Stokes equations of motion, after making the

following simplifying assumptions:

(i) that the familiar boundary layer approximation holds, i.e. the radial velocity component is very much smaller than the tangential one;

(ii) that the ratio of the width of the flow to the radius of the flow curvature is very small

$$\text{i.e. } \frac{y}{R_0} \sim O(\delta) \quad \text{and} \quad \frac{1}{R_0+y} \sim \frac{1}{R_0}$$

(iii) that the pressure changes in the flow direction are negligible in so far as they affect the momentum of the flow;

(iv) that the velocity profiles are similar and the boundary layer portion of the flow is negligible, and that the non-dimensional velocity profiles can therefore be represented by a half free jet profile;

(v) that the rate of spread of the jet is proportional to v' , which in turn is proportional to the centrifugal pressure across the flow, the constant of proportionality being established experimentally;

(vi) that the turbulent shear stress can be simply related to eddy viscosity as was done by Gortler for a free jet;

(vii) that all self preservation of $\overline{u'^2}$ and $\overline{v'^2}$ exists as stipulated by Townsend (Ref. 9).

(viii) that all flows can be reduced to a universal flow which emanates from hypothetical origin.

Assumptions (i) and (viii) are the same as, (ii) and (iii) are simpler than, and (iv), (v), (vi) and (vii)

are different from Newman's assumptions.

Nakaguchi found that the velocity profile he assumed (half a free jet) agreed fairly well with the experimental results except in the minor part close to the wall surface.

He theoretically developed the relationship for jet growth

$$\frac{y_{m/2}}{R_0} = 0.04\theta^2 + 0.086\theta \quad (2.11)$$

which agreed well with his experimental results.

The jet growth law given by Nakaguchi deviates rapidly from that given by Newman for θ values larger than about 160° . Nakaguchi also derived the formula for the local maximum jet velocity

$$\frac{u_m}{(u_m)_1} = \left[\frac{y_{m/2}}{(y_{m/2})_1} \right]^n \quad (2.12)$$

where $(u_m)_1$ was the maximum jet velocity at some arbitrarily chosen point in the fully developed flow. This prediction is fairly satisfactory except in the vicinity of the jet slot where the potential core remains. The value of n is little smaller than -0.5 .

The static pressure on the wall is given by

$$\frac{P_a - P_s}{\frac{1}{2}\rho U_0^2} = 1.51 \left(\frac{u_m}{U_0} \right)^2 \frac{y_{m/2}}{R_0} \quad (2.13)$$

The theoretical values are slightly greater than the experimental ones. In a general all the theoretical methods predict the surface pressure distribution not as well as other quantities.

2.5 GAP EFFECT

In 1962, Korbacher (Ref. 6) investigated gap effect on a curved wall jet by measuring the forces and pressure acting on a quadrant. He found that the Coanda phenomenon was also effective when the deflection surface was separated from the nozzle by a wide gap open to the atmospheric pressure. The experiments were carried out for nozzle pressure ratios up to and well above the critical. Gaps along the nozzle axis of up to eight times the jet sheet thickness (at $Ro = 2.5$) have practically no effect on the component of the force in the direction normal to the nozzle axis. Maximum b' (at any given l') for which the jet was able to bridge the gap depended on the jet slot thickness. The larger the jet sheet thickness, the smaller the b' gaps. He concluded that the effect of the l' gap size on the static pressure distribution on the wall was small. He also observed the hysteresis phenomenon associated with the gap perpendicular to the nozzle axis (explained in section 4.2). These findings were confirmed by Benner's (Ref. 8) investigation which was a continuation of the work reported by Korbacher.

Tu (Ref. 7) in his experimental study of gap effect on a plane wall jet flow found that only the flow in the region close to the leading edge of the wall was affected by the gap. The length of this region which depended on the gap size, was so small for

small gaps that the gap effects were negligible.

CHAPTER III

TEST FACILITIES

The apparatus is shown in Figures 1,3,4, and 5. References to the letter code used in Fig.1 are made in the description of the test facilities.

3.1 AIR SUPPLY AND GUIDING DUCT

Air was supplied by a type HS, size 200 American Standard centrifugal fan (A) with static pressure of 5 inches water. This fan was driven by a 5 h.p., 1745 r.p.m. General Electric induction motor. A 30 inch long, wooden guiding duct (B) with a rectangular cross section was attached to the fan exit. A honeycomb flow straightener was placed in the guiding duct to reduce the turbulence level induced by the fan.

3.2 CONTRACTION DUCT AND NOZZLE

A wooden contraction duct (C) 30 inches long was placed after the guiding duct. A converging nozzle (D) made of brass with a 0.25" x 9" exit was attached to the contraction duct. The contraction ratios for the nozzle together with the duct were 62:1 in the direction of 0.25" width and 2.5:1 in the perpendicular direction. A Kiel probe with a 0.125" diameter shroud was placed

in the contraction duct to measure air supply pressure.

3.3 WALL AND TRAVERSING MECHANISM

The curved wall (E) consisted of a 9" long half cylinder made of smooth plexiglass. The outside diameter of the cylinder was 12 inches. Twenty-nine static pressure taps of 0.040" diameter were drilled 1.5" away from the centre line in order to eliminate their effect on the jet probing.

A piece of 30" x 40" x 0.25" plexiglass plate on the top and a combination of rolled steel plate and plexiglass plate at the bottom were used as end plates to obtain the two dimensional flow condition. The wall (E) was mounted perpendicular to the endplates with the 9" direction being parallel to the spanwise direction of the jet slot.

The mechanism used for moving the wall to the required gap position, was capable of moving the wall both parallel and perpendicular to the jet. In both the directions, distances could be measured to an accuracy of 0.005".

The traversing mechanism was provided with leveling screws to ensure correct alignment with the nozzle exit.

3.4 PROBING EQUIPMENT

A flattened stainless steel hypodermic tube (Fig.3)

with an opening of 0.005" x 0.060" was used to measure the total pressure in the jet. A similar hypodermic tube of the same outer dimensions with slots on the narrow sides (Fig.3) was used for static pressure probing. These probes were mounted on a specially designed apparatus which moved the probes in the radial direction with an accuracy of ± 0.001 inch. A multi-tube inclined manometer with an accuracy of ± 0.01 inch of water was utilized in making all pressure measurements.

CHAPTER IV

EXPERIMENTS

Throughout the experiment, the nozzle width, the jet velocity at the nozzle exit and the radius of the cylinder were kept constant. The size of the gap was the important variable. The flow was two dimensional because of the end plates. The Reynolds number for the experiment was 6.4×10^4 ($Re = \left[\frac{(P_T - P_a) R_o t}{\rho \nu^2} \right]^{\frac{1}{2}}$).

4.1 CALIBRATION

The flattened hypodermic tube used for measuring the total pressure was compared with a small Kiel probe under actual test conditions. The results indicated a very good agreement.

The specially designed static pressure tube was compared with a standard probe in a wind tunnel. A very good relationship was obtained as shown in Fig.6. These two flattened tubes were expected to give good results in the velocity and pressure gradients because of the narrow openings.

The velocity distribution across the width of the nozzle exit at different positions along the span of the nozzle were determined. No significant changes in these distributions were noted. The velocity distribution was

found to be effectively uniform over 85% of the 0.25" width varying only $\pm 1\%$ from the central core velocity of 145 ft/sec.

Two dimensionality check was done by investigating the velocity profiles at stations 1.5" above the centre line, centre line and 1" below the centre line for no gap at $\theta = 90^\circ$. All these velocity profiles overlapped (Fig. 7) and therefore the flow was considered to be two dimensional.

4.2 HYSTERESIS

For any gap l' , when the curved surface was moved away from the jet (b' increased), at a particular value of b' (say b'_D) the jet sheet detached from the surface. But when the curved surface was brought back (b' reduced) the jet attached to the curved surface at a different value of b' (say b'_A). Because of the jet inertia, $b'_A < b'_D$. At different values of l' these "attached" and "detached" positions were noted. This information (Fig.8) was also useful for determining the range of gap sizes for other experiments.

4.3 WALL PRESSURE MEASUREMENTS

The curved wall was installed between the two end plates and the leading edge was sealed against the nozzle exit. The static pressure distribution along the curved surface was measured with the static taps on the wall connected to an inclined tank.

By means of the traversing mechanism the wall was moved away from the nozzle exit to get the desired values of λ' and b' .

The different gaps were obtained by keeping the leading edge of the curved wall:

1. on the approximate boundary of the free jet for $\lambda'=3, 8$ and 12 .
2. on attached positions (see Fig. 8) for $\lambda'=0, 1, 3, 6, 9$ and 12 .
3. on a line defined by $\lambda'=8$ with values of $b' = 0.56, 2, 2.64$ and 3.56 .

The wall pressure distribution was measured for the above gap positions.

4.4 MEASUREMENT OF JET VELOCITY

The two-dimensional curved wall jet with and without gap was probed at four or more stations along the jet, i.e., at different values of θ . The static and total pressure probes were placed at a distance of 0.5" above and below the centre line of the flow surface respectively. The radial distance between two consecutive probing points was varied from 0.003" to 0.1" depending upon the local jet thickness and the proximity to the wall.

For the jet probing experiments the different gaps were obtained by keeping the leading edge of the curved wall on the approximate boundary of the free jet (see Fig.9) for $\lambda' = 2, 4, 8$ and 12 .

4.5 VISUALIZATION OF FLOW SEPARATION

A mixture of lamp black and kerosene was applied to the bottom end plate and to the curved surface of the wall (Fig.10) to determine the angular position of separation. Both methods gave the values for θ_{sep} . independently and results had a reasonable agreement (a difference of about three degrees).

In the region of the curved surface where the flow was attached, the motion of lamp black particles were influenced by two factors, namely, the jet flow and the pull of gravity. In the region after the flow separation, the lamp black particles were not affected by the jet flow and hence the particle traces were vertical (Fig.11). The location of the first vertical trace gave the position of the flow separation.

The values of θ_{sep} . were determined for the curved wall jet with different gaps. In the first set of gaps, the leading edge was moved along the free jet boundary. In the second set of gaps b' was changed while keeping l' constant. This was done for three different values of $l' = 4, 8$ and 12 .

CHAPTER V

EXPERIMENTAL RESULTS

5.1 DATA REDUCTION

The fluid was treated as incompressible because the maximum jet velocity was only 145 ft/sec. From barometric pressure and room temperature, the density of air was determined. The experimental data was reduced with the help of an IBM 1620 computer. Input data were room temperature, barometric pressure, surface pressure tap locations and readings, radial positions and pressure readings from jet probing, U_0 , θ , l , b , R_0 and t . The values of u , u_m , y_m , $y_{m/2}$, $\frac{u}{u_m}$, $\frac{y}{y_{m/2}}$, $\frac{u_m}{U_0}$, $\frac{y_{m/2} - y_m}{t}$, $\frac{(P_a - P_s)R_0}{(P_T - P_a)t}$, s' , $\frac{y_{m/2}}{R_0\theta}$, $\frac{y_{m/2}}{R_0}$ and the force acting on the surface were obtained as output information.

5.2 PRESENTATION AND DISCUSSION OF RESULTS

5.2.1 HYSTERESIS

Figure 8 shows the "attached" and "detached" positions for different values of l' and the approximate free jet boundary. It is seen that the difference between the values of b' for "detached" and "attached" positions, m' , first decreases slowly and then rapidly as l' increases. It is interesting to note that three lines in Fig. 8

come close together as l' is increased.

Further, it was observed during the experiments that for large values of l' ($l' \approx 16$) the deflection of the jet by means of the curved surface was not very stable. This may be explained by the fact that the value of m' was small.

From the surface pressure measurements the values of the component of the force acting on the surface in the direction of the nozzle axis were calculated for different gaps. It appeared that this force component was maximum close to the attached line.

5.2.2 VELOCITY PROFILES

The non-dimensional velocity profiles at different stations along the curved wall jet without a gap are shown in Fig. 12. It is seen that the experimental results closely follow the theoretical velocity profile of a plane wall jet given by Glauert (Ref. 1). This agreement was also noted previously by Newman (Ref. 2) and Fekete (Ref. 5). However, in the present investigation it is observed that for the angles $\theta = 30^\circ$ and even for 60° the velocity profile is not settled and deviates from the Glauert's theoretical velocity profile for a plane wall jet. For $\theta = 90^\circ$ and 120° the experimental profiles agree very well with the theory. It is worth noting that the experimental non-dimensional velocity profile of a plane wall jet (Ref. 7) almost

coincides with that of the curved wall jet for small values of θ ($\theta = 30^\circ$ as seen from Fig. 12). This might be because the effect of Coanda deflection is negligible for small values of θ and therefore the dimensionless velocity profile for curved wall jet initially has a tendency to attain the plane wall jet velocity profile. In the case of large θ values when the effect of flow turning becomes appreciable the profile approaches the Glauerts theory for "plane wall" jet.

Plots in Fig. 13 show the non-dimensional velocity profiles at different stations along the curved wall jet with different gaps obtained by keeping the leading edge of the wall on the jet boundary. In the region close to the leading edge of the wall, the velocity profiles (Fig. 13) are not similar. This is because of the change in the initial condition of the jet caused by the gap size. It is clearly seen that the velocity profile settles down as the jet flows along the curved wall and ultimately becomes the same as that for no gap. Similar effect on velocity profiles was observed by Tu (Ref. 7) in case of a plane wall jet.

The non-dimensional velocity distribution in the outer layer of the curved wall jet with and without a gap could be expressed in the following way:

$$\frac{u}{u_m} = f \left[\frac{y - y_m}{y_{m/2} - y_m} \right] \quad (5.1)$$

These plots are shown in Fig. 14. We observe that the outer profile for a curved wall jet with and without an initial gap is similar to one half of a free jet profile.

Dimensional velocity profiles at $\theta = 30^\circ$ for the gaps along the the jet boundary are shown in Fig. 15. It is seen that the values of maximum velocity as well as the shape of the profile at a given θ position changes with λ' .

The static pressure distributions in the jet for no gap are plotted in Fig. 16. These are in agreement with other available experimental results (Refs. 2 and 3).

5.2.3 JET GROWTH

The effect of an initial gap on the growth of the jet flow over the curved wall is obtained from the plots of $\frac{y_{m/2}}{t}$ vs. s' (Fig. 17). The value of $\frac{y_{m/2}}{t}$ is higher than the value for the curved wall jet without a gap, the difference increasing with increasing gap size. However, for any given gap size, the difference decreases downstream from the leading edge and finally tends towards a constant value, i.e., the rate of change of $\frac{y_{m/2}}{t}$ with s' equals the zero gap rate.

Figure 18 shows the growth of the outer layer of the jet. We see that the initial gap has practically no effect on the growth rate of the outer layer the curves in Fig. 18 are almost parallel. Further, the distance along the s' axis between the growth lines is approximately equal to the difference in \mathcal{L}' values of the curves. In other words, these plots would collapse into one line if the distances along the flow were measured from the nozzle exit instead of the leading edge of the wall.

Tu (Ref. 7) in his investigation of the gap effect on a plane wall jet observed that the growth rate of the outer layer was influenced by the gap size. The difference between plane and curved wall jets in this aspect is worth noting.

For large gaps ($\mathcal{L}' = 4, 8$ and 12) the inner layer thickness decreases rapidly in the beginning and then increases as the jet flows along the surface (see Fig. 19). The rate of change of $\frac{y_m}{t}$ with s' for any given gap tends towards the zero gap rate. The shift of the maximum velocity point is due to the effect of the wall drawing the jet closer, which is caused by the difference in shear stresses acting in the inner and outer layer. Fig. 19 clearly indicates that the region close to the leading edge of the wall is a settling region, where the jet changes from a free jet to a curved wall jet. Qualitatively stating, the length of this settling

region depends on the size of the gap. It is also noted that for a given gap size, the settling length required is smaller in the case of curved wall jet than that of plane wall jet.

Figure 20 gives the streamwise variation of $\frac{y_{m/2}}{R_0\theta}$ with $\frac{y_{m/2}}{R_0}$ for the gaps along the jet boundary (see equation 2.9). Table I gives the constants of the present investigation and also the results of earlier investigations. It is seen that the effect of initial gap is large near the leading edge and diminishes as θ increases.

5.2.4 MAXIMUM VELOCITY DECAY

The maximum velocity decay of curved wall jets with different gaps are shown in Fig. 21. It is seen that the rate of decay is initially less for gaps than for no gap but eventually the gap effect on the decay rate diminishes.

The decay plots of the type used by Newman and Fekete (Refs. 2 and 5) are given in Fig. 22. Agreement between Fekete's results and the present investigation is good.

5.2.5 SURFACE PRESSURE DISTRIBUTION

The surface pressure coefficient C_p measured on the cylinder is plotted against the angular position θ in Figure 23. After disregarding the irregular pressure

134567

UNIVERSITY OF WINDSOR LIBRARY

distribution near the leading edge of the wall (say $\theta < 20^\circ$) it is noted that the pressure difference across the jet initially increases with the gap size because of the larger jet thickness. But after the jet flows through some angle, the pressure difference and hence C_p reduces more rapidly for larger gaps causing earlier separation. The same phenomenon is observed for the gaps along jet boundary, gaps along attached line and gaps perpendicular to the axis of the nozzle.

Since the information obtained on separation point from the pressure distribution is only qualitative, the $\theta_{sep.}$ is determined from flow visualization studies.

5.2.6 SEPARATION

If the curved surface had been a full cylinder ($\theta_{max.} = 360^\circ$), then the separation would have occurred at 240° for no gap (Ref. 2). But half cylindrical surface being probably more useful for practical applications, was selected. For a half cylinder without a gap, the separation would naturally take place close to the trailing edge of the surface, i.e., $\theta_{sep.} \approx 180^\circ$. The decrease in $\theta_{sep.}$ with gap size for gaps along the jet boundary and along the attached line plotted is shown in Fig. 24. It is seen that a gap appreciably reduces the $\theta_{sep.}$ Figure 25 gives the plots of $\theta_{sep.}$ vs. b' for values of $\lambda' = 4, 8$ and 12 . It is evident that $\theta_{sep.}$ depends both on λ' and b' , larger the value of λ' and b' ,

smaller the angle θ_{sep} .

CHAPTER VI

CONCLUSIONS

6.1 CURVED WALL JET WITHOUT A GAP

1. Velocity profiles are similar except near the leading and trailing edges.

2. Non-Dimensional velocity profile agrees well with Glauert's theoretical plane wall jet profile for $\alpha = 1.2$.

3. The jet growth could be described by the following equation:

$$\frac{y_{m/2}}{R_0 \theta} = C + C k \frac{y_{m/2}}{R_0}$$

where $C = 0.11$ and $k = 1.67$.

4. For a half cylinder, θ_{sep} is approximately equal to 180° .

5. Measured surface pressure coefficient C_p is less than the theoretical value of 2 and decreases to zero near the trailing edge.

6.2 CURVED WALL JET WITH A GAP

1. The curved wall jet flow in a region close to the leading edge of the wall is affected by the gaps. In this region velocity profiles are not similar and the rates of the jet growth and the maximum velocity decay

change from point to point along the length of the jet and eventually tend towards the no gap rates.

2. The region affected by the gap is described as the settling region where the type of flow changes from a free jet to a wall jet.

3. The settling length increases with the gap size. For a given gap size, the settling length of a curved wall jet is less than that of the plane wall jet.

4. The flow in the outer layer of the curved wall jet is not affected by a gap.

a) The outer layer velocity profile is similar to that of a free jet profile.

b) The outer layer growth rate is not affected by an initial gap.

5. The pressure difference across the jet initially increases with the gap size. However, after the jet flows through some angle, the pressure difference and hence C_p reduces more rapidly for larger gaps causing earlier separation.

6. The value of angular position of separation decreases with an increase in gap size.

7. There is hysteresis phenomenon associated with gaps. As the value of ζ increases, the "attached" line, "detached" line and jet boundary come closer together and the jet deflection by means of the curved surface becomes less stable.

REFERENCES

1. Glauert, M.B. The Wall Jet. J. Fluid Mech.,
Volume 1, P. 625, (1956).
2. Newman, B.G. The Deflection of Plane Jets by
Adjacent Boundaries - Coanda Eff-
ect. Boundary Layer and Flow
Control, Vol. 1, Edited by G.V.
Lachman, Pergaman Press, P. 232,
(1961).
3. Nakaguchi, H. Jet Along a Curved Wall. Dept.
of Aeronautics, University of
Tokyo, Research Memo No. 4 (1961).
4. Sawyer, R.A. Two-Dimensional Turbulent Jets
with Adjacent Boundaries. Cam-
bridge University, Ph.D. Thesis,
(1962).
5. Fekete, G.I. Coanda Flow of a Two Dimensional
Wall Jet on the Outside of a
Circular Cylinder. McGill Univ-
ersity, Report No. 63 - 11. (1963).
6. Korbacher, G.K. The Coanda Effect at Deflection
Surfaces Detached from the Jet
Nozzle. Can. Aeronautics and
Space Journ., Vol. 8, No. 1,
(Jan. 1962).
7. Tu, P.K.C. An Experimental Investigation of
the Flow in a Plane Wall Jet
with an Initial Gap. M.A.Sc.
Thesis, Dept. of Mech. Eng.,
University of Windsor, (1965).
8. Benner, S.D. The Coanda Effect at Deflection
Surfaces Widely Separated from
the Jet Nozzle. UTIAS Technical
Note No. 78, (April, 1965).
9. Townsend, A.A. The Structure of Turbulent Shear
Flow. Cambridge University
Press, (1956).

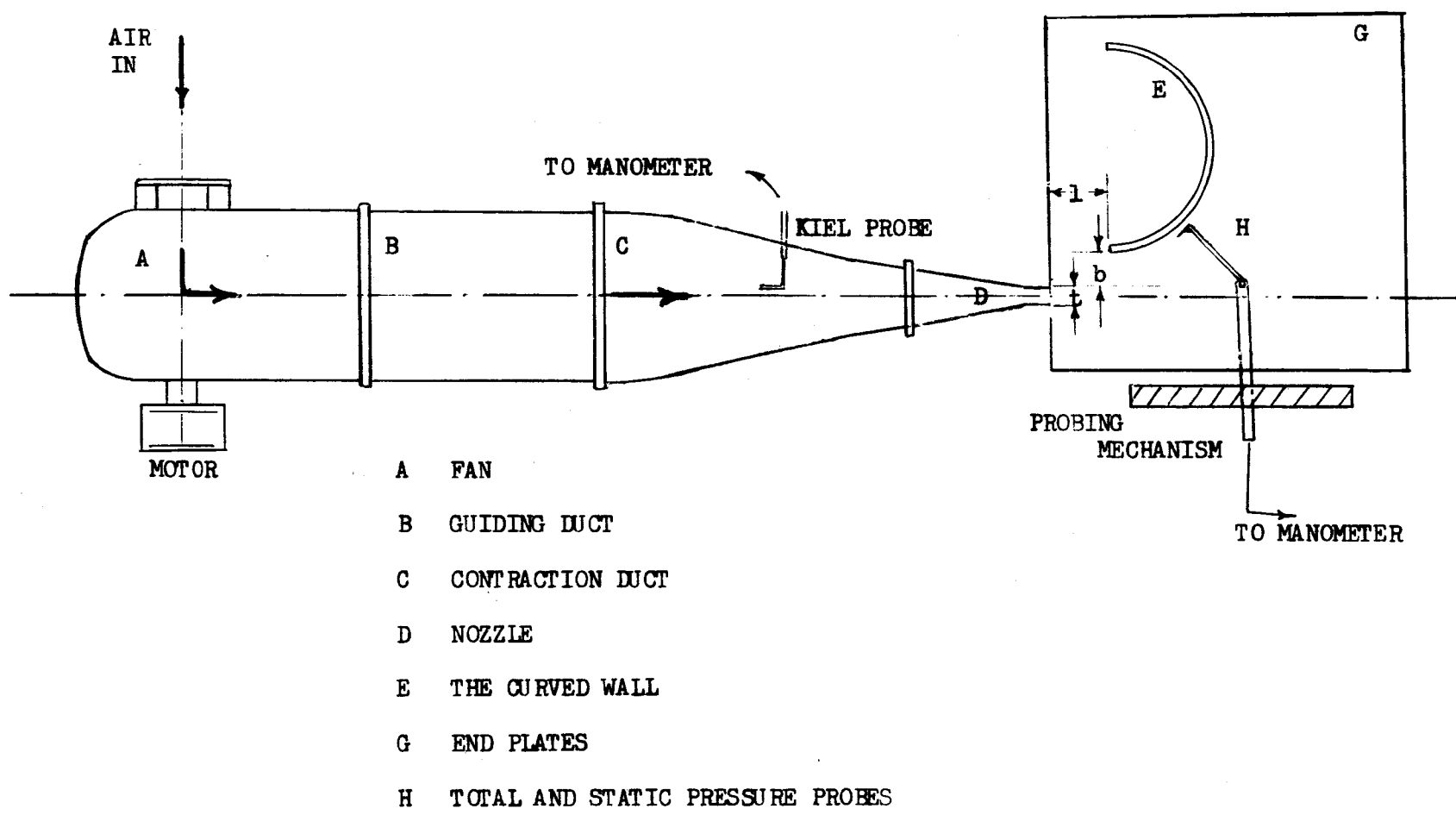


Fig. 1 SCHEMATIC DIAGRAM OF TEST FACILITIES

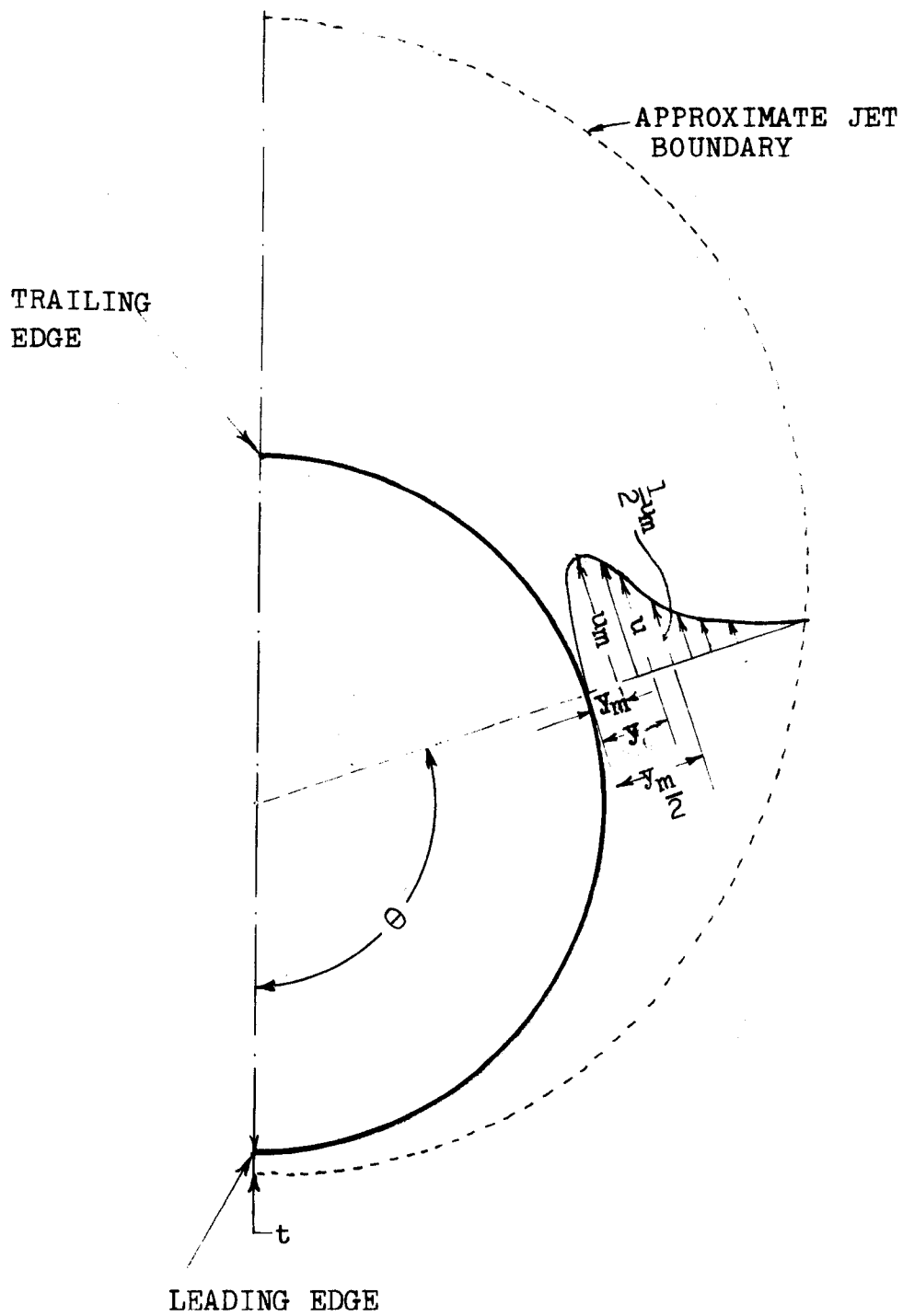


Fig. 2 CURVED WALL JET NOMENCLATURE

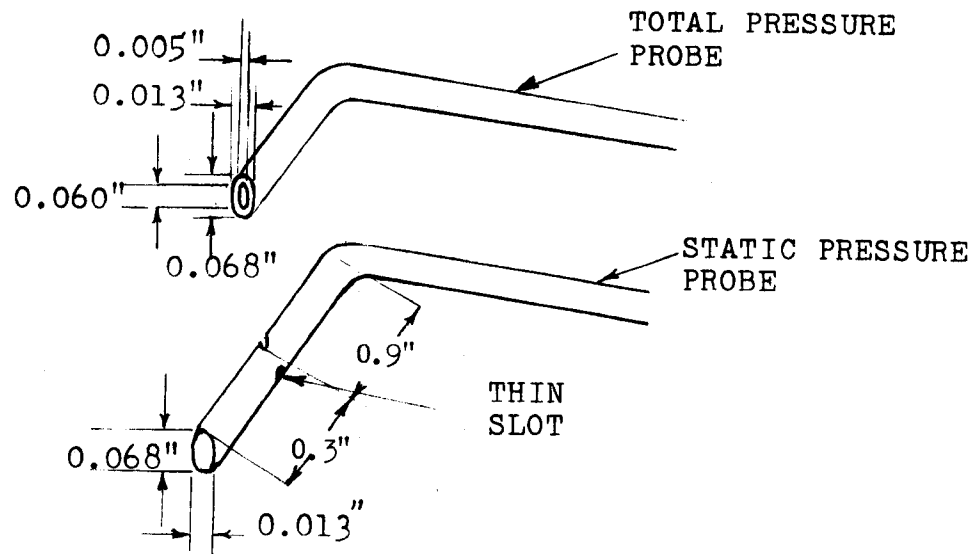


Fig. 3 STATIC AND TOTAL PRESSURE PROBES

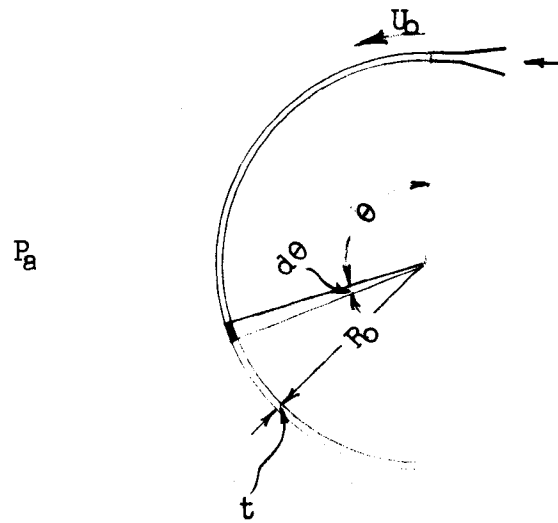


Fig. 4 FLOW PICTURE FOR NON -VISCIOUS THEORY

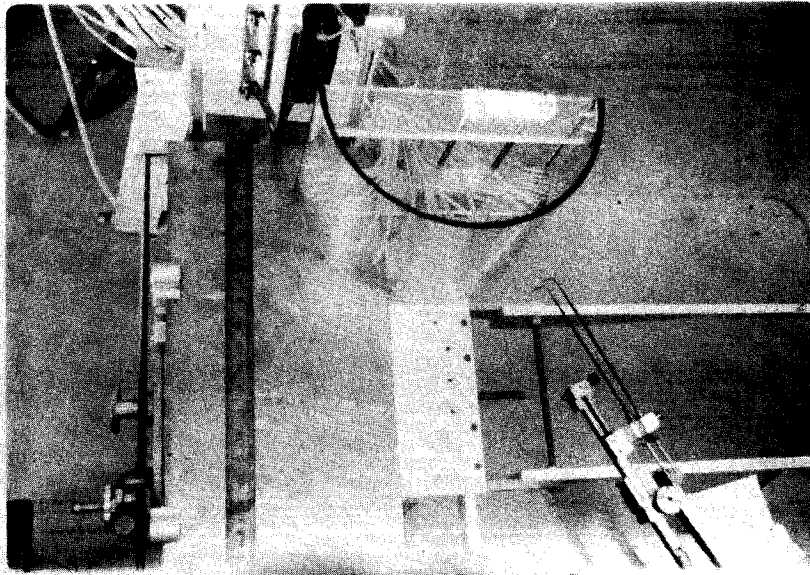


Fig. 5.a

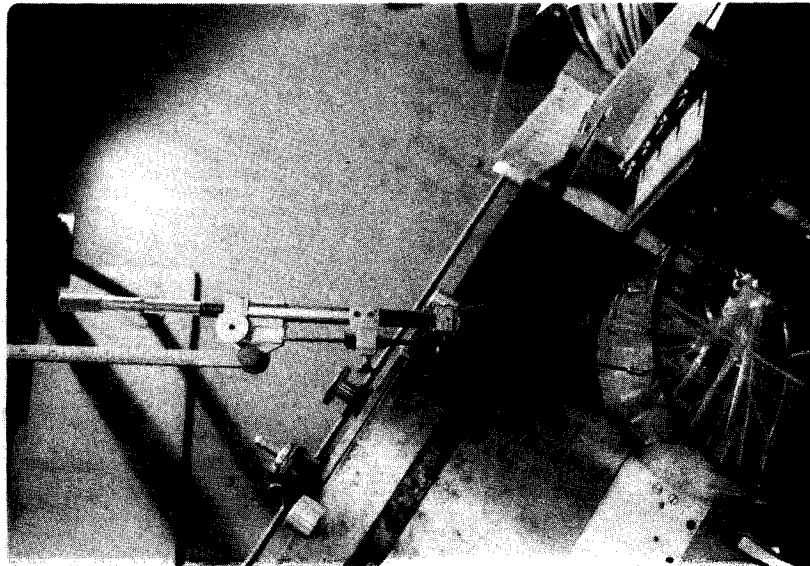


Fig. 5.b

Fig. 5 VIEW OF EXPERIMENTAL ARRANGEMENT

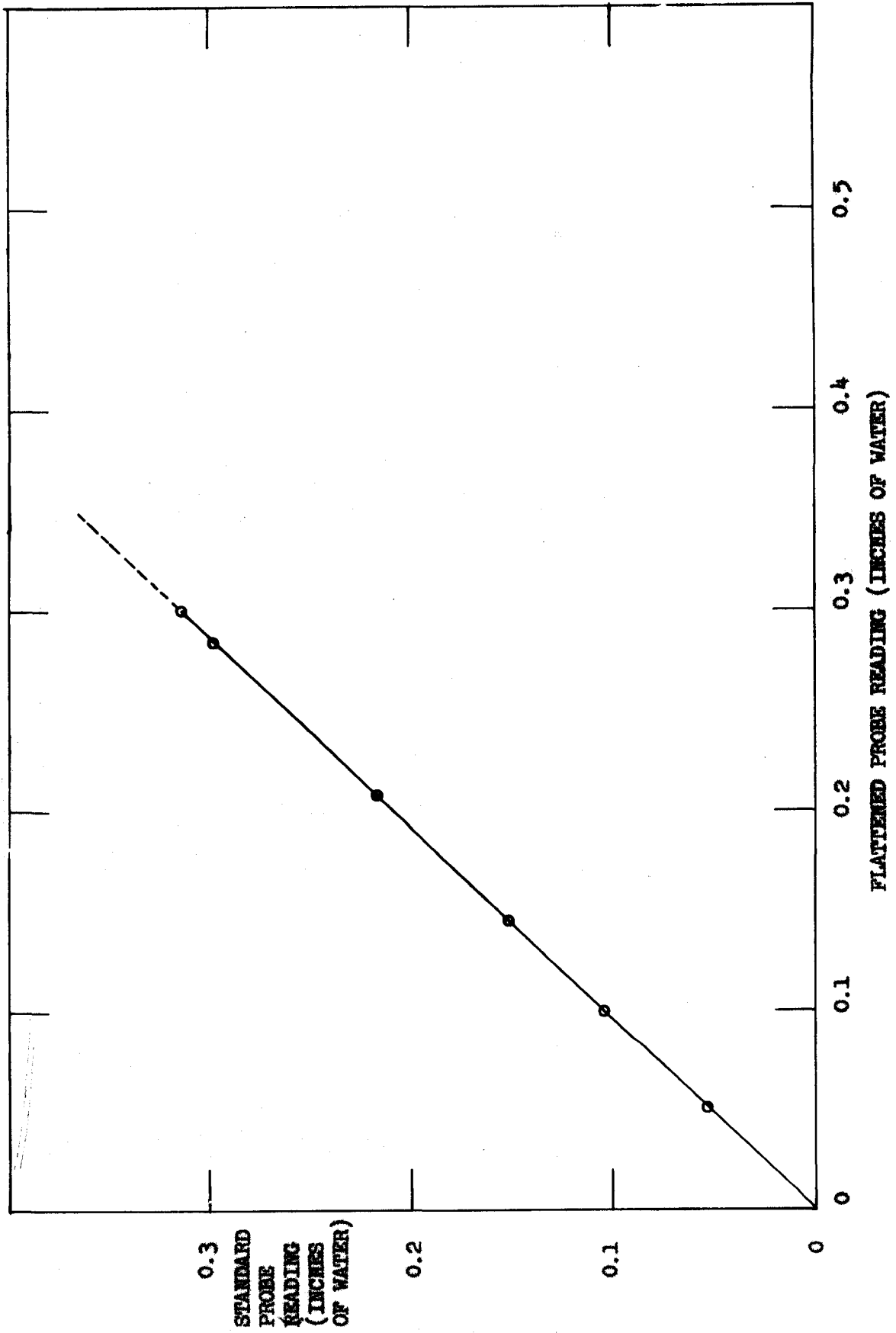


Fig. 6 STATIC PRESSURE PROBE CALIBRATION

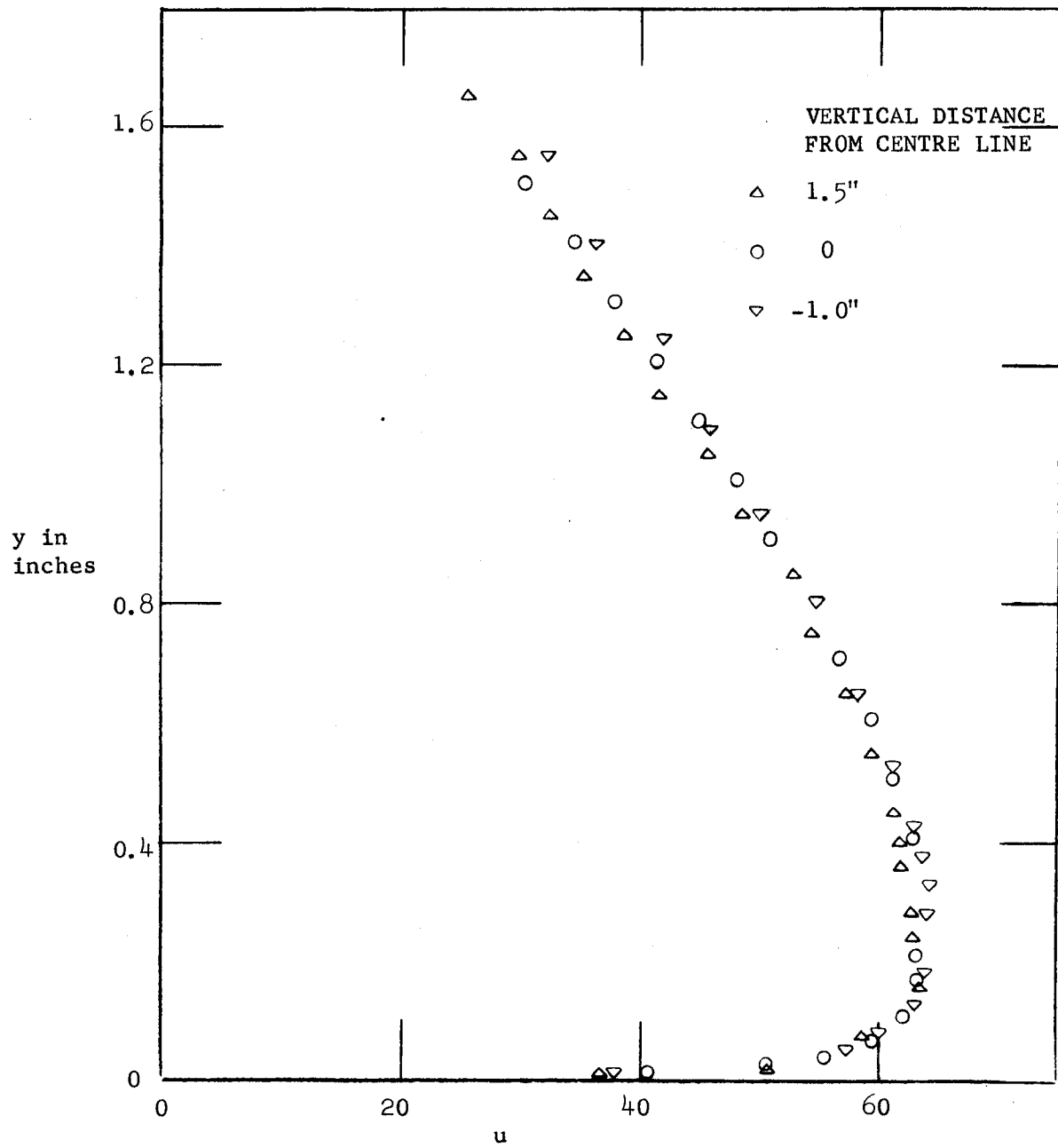


Fig. 7 TWO DIMENSIONALITY CHECK

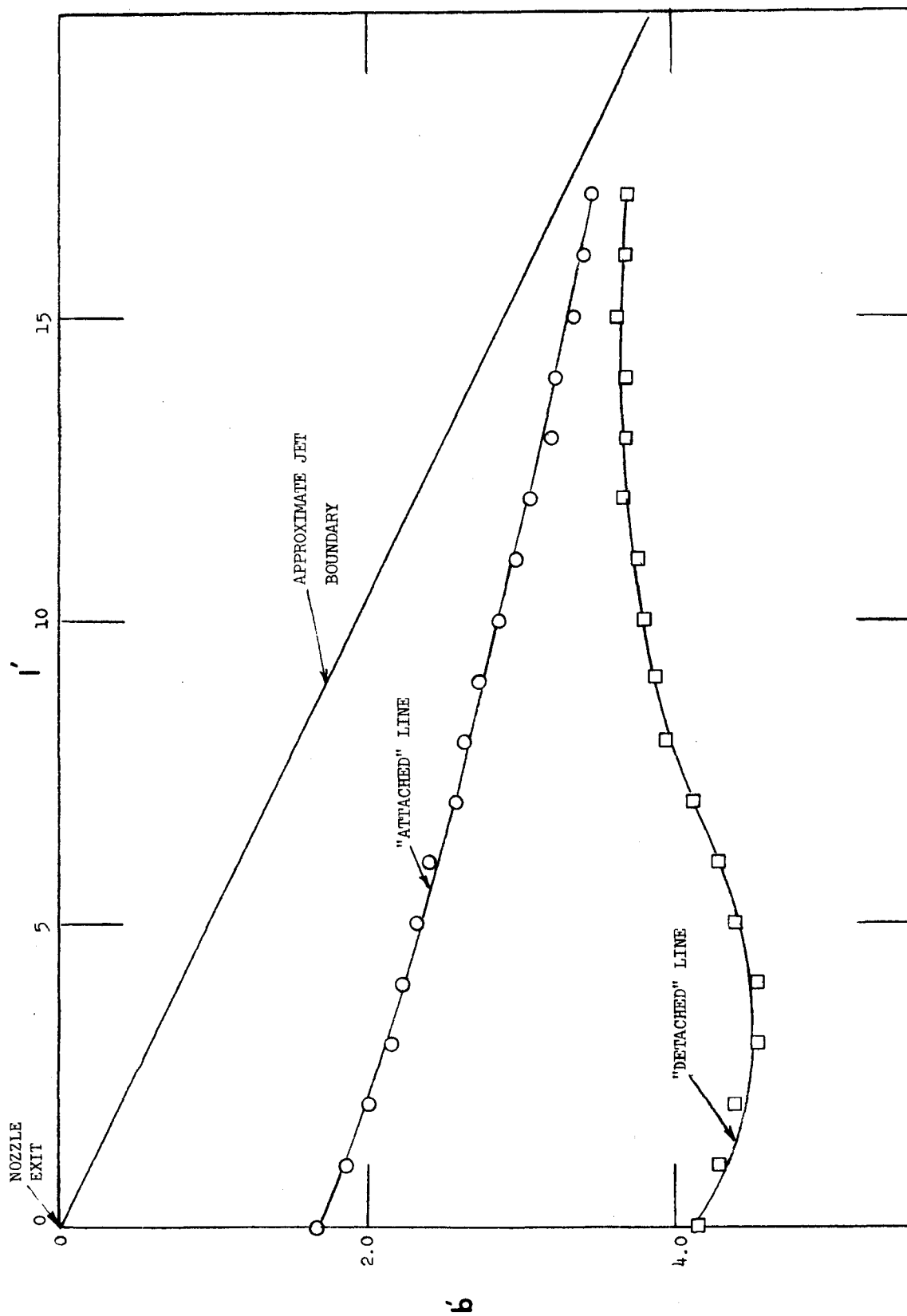


FIG. 8 HYSTERESIS PLOTS

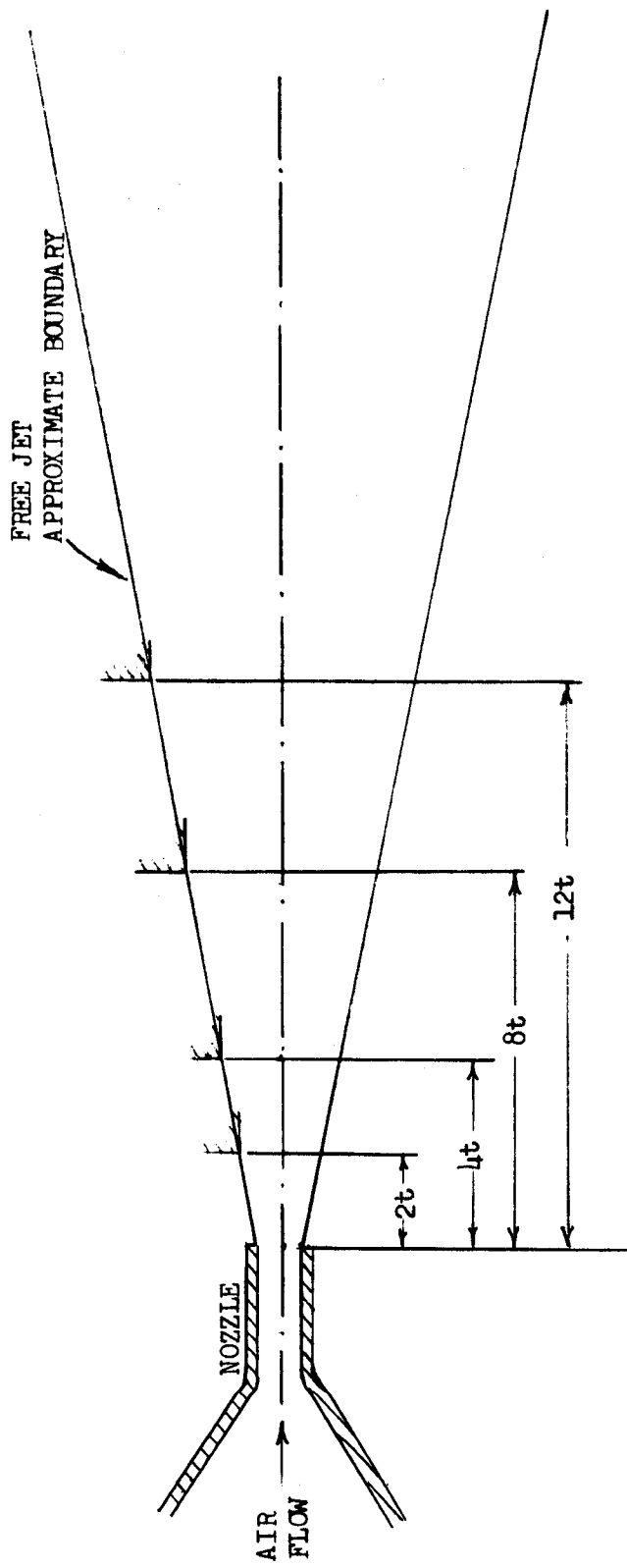


Fig. 9 LEADING EDGE POSITION ALONG THE JET BOUNDARY



a. ON BOTTOM END PLATE



b. ON THE CURVED WALL SURFACE

Fig. 10 VISUALISATION OF FLOW SEPARATION

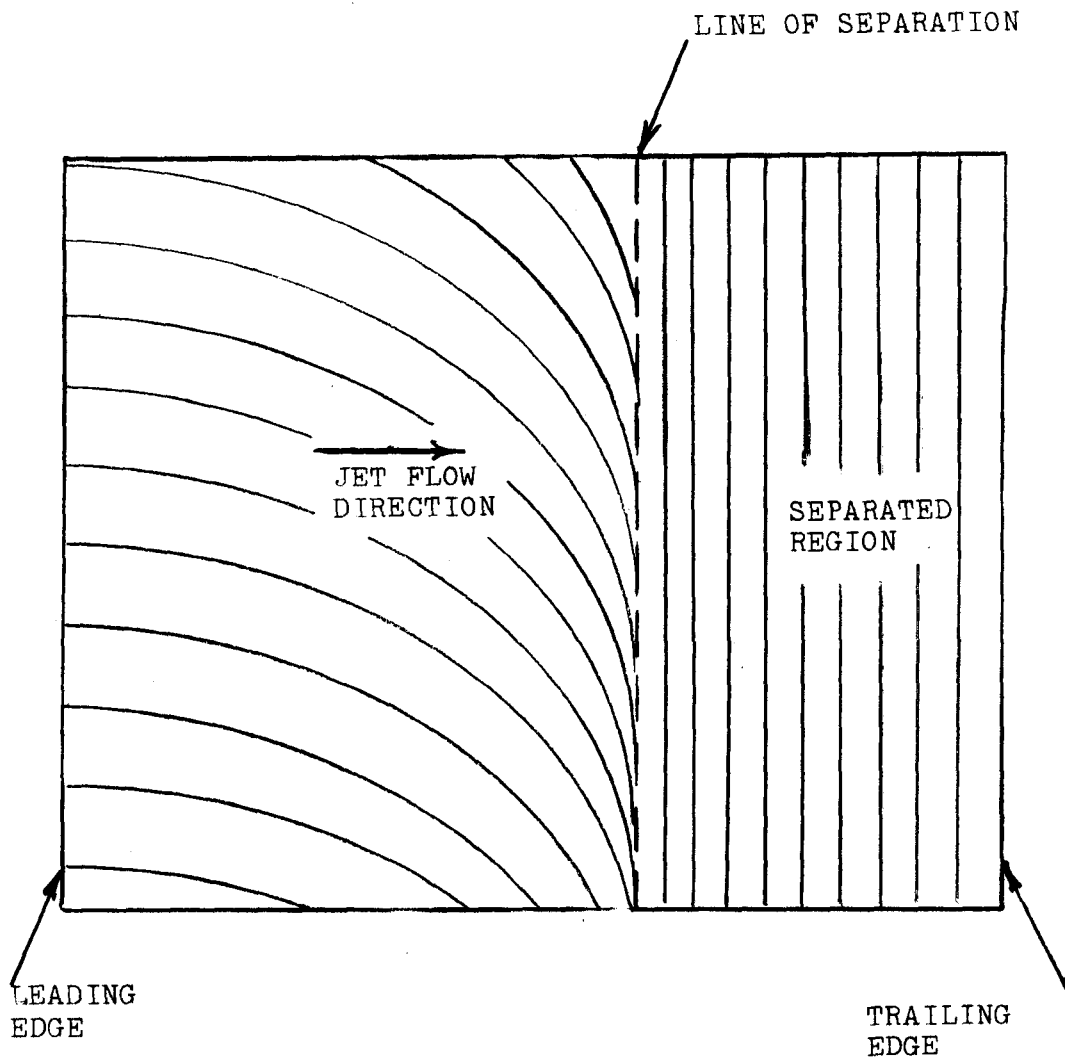


Fig. 11 SKETCH OF LAMP BLACK TRACES ON CURVED SURFACE

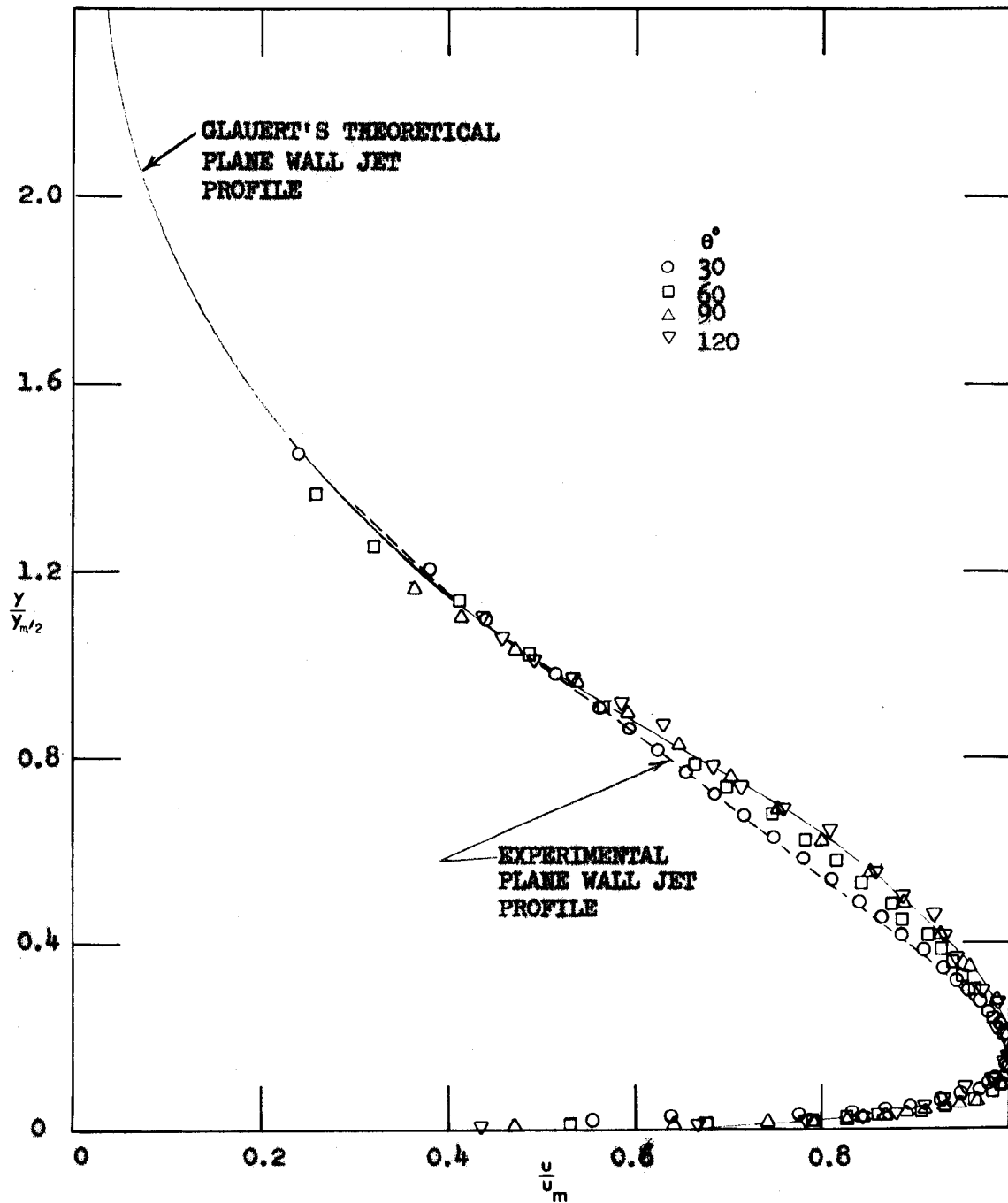


Fig. 12 NON-DIMENSIONAL VELOCITY PROFILE OF CURVED WALL JET WITHOUT A GAP

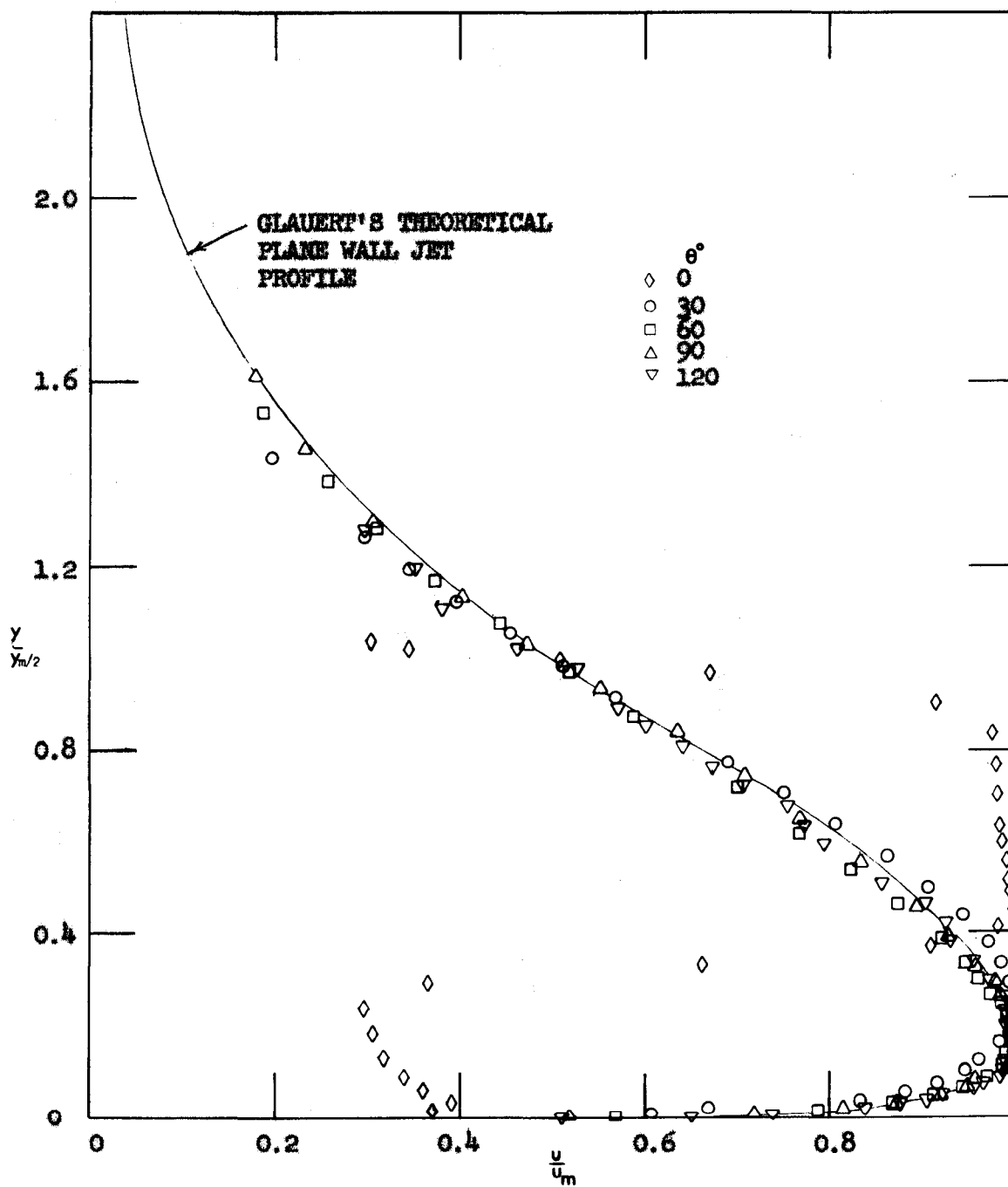


Fig. 13 NON-DIMENSIONAL VELOCITY PROFILE OF CURVED WALL JET WITH GAPS ALONG JET BOUNDARY

a. $\lambda' = 2$

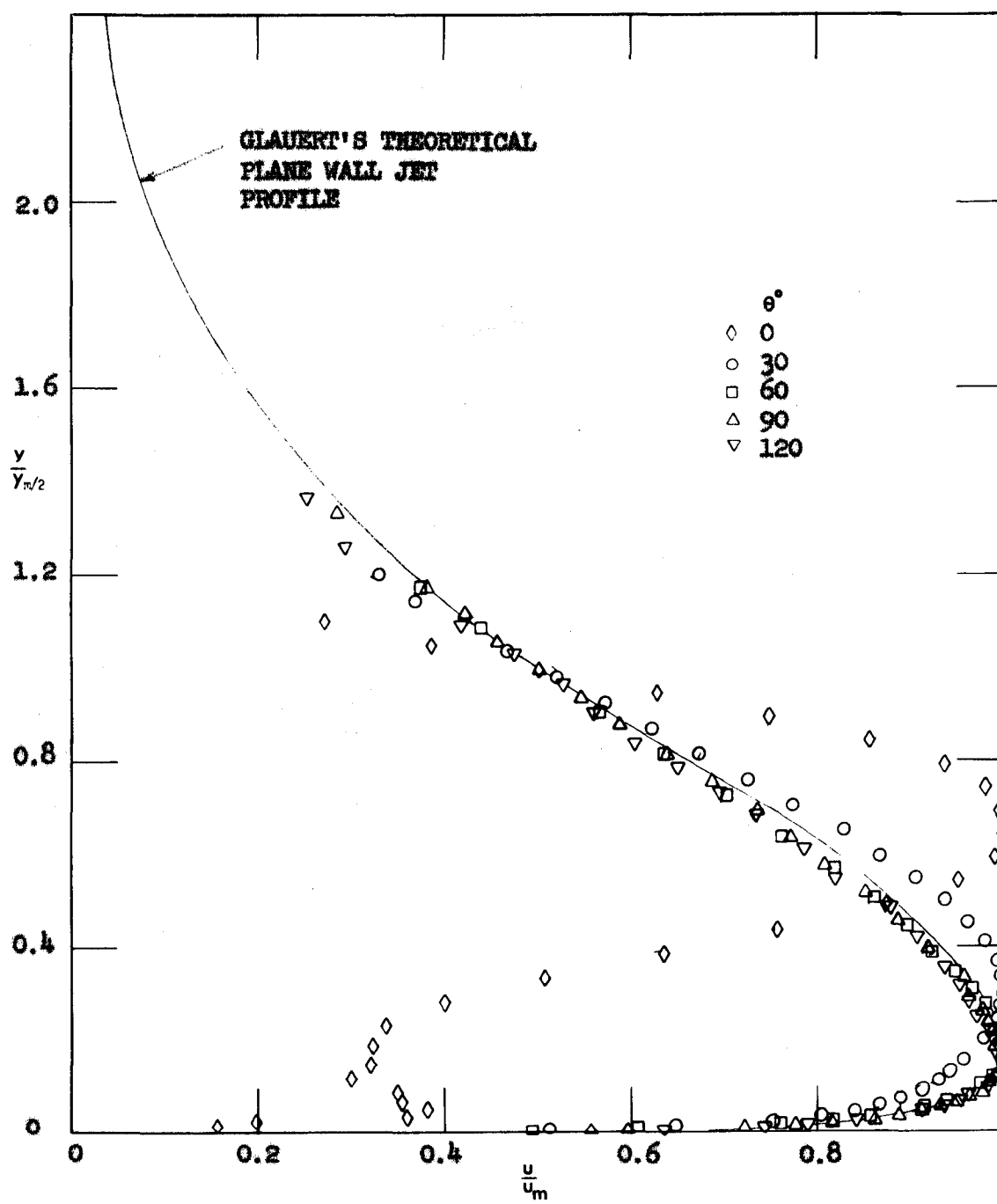


Fig. 13 b. $l=4$

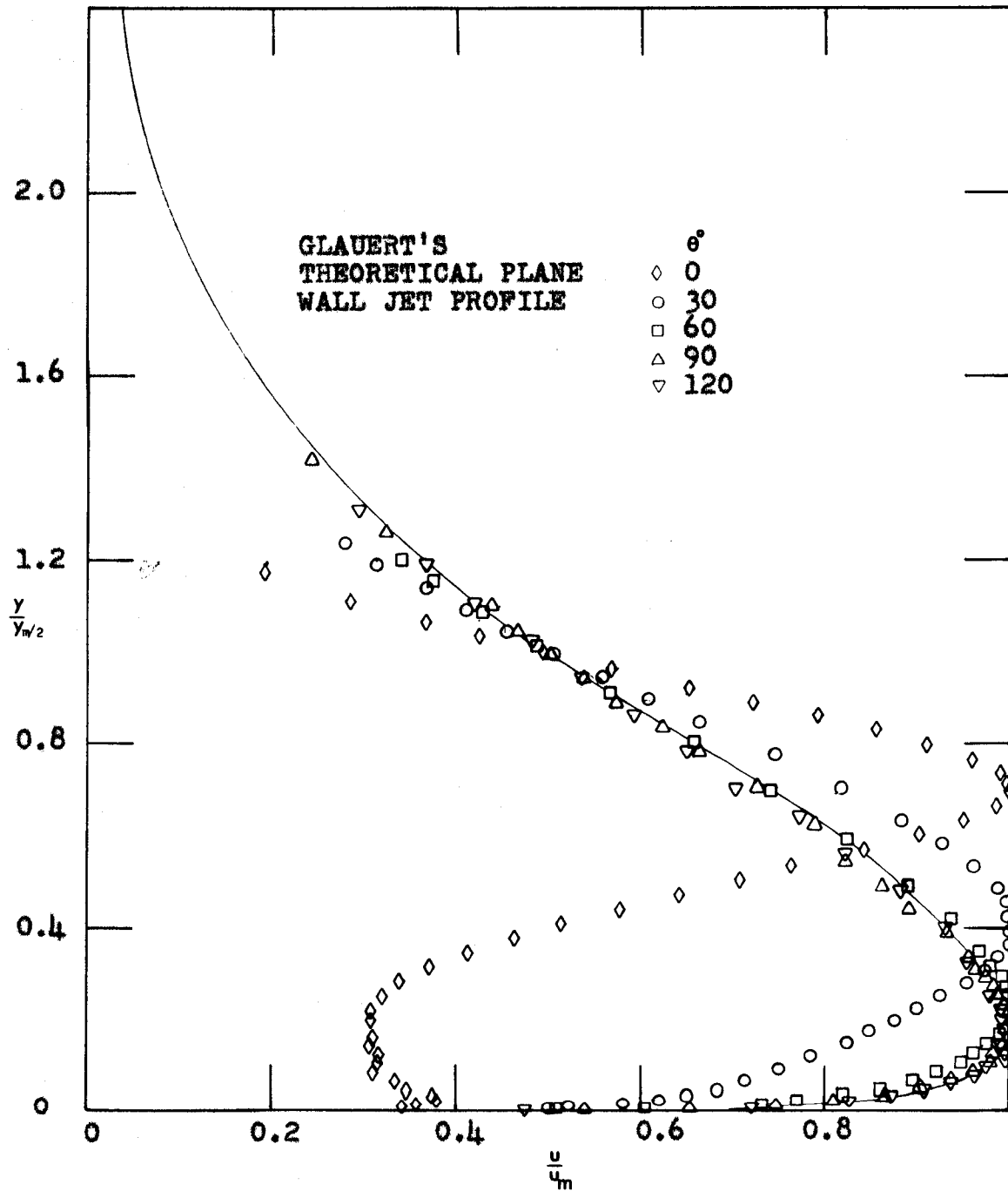


Fig. 13 c. $l' = 8$

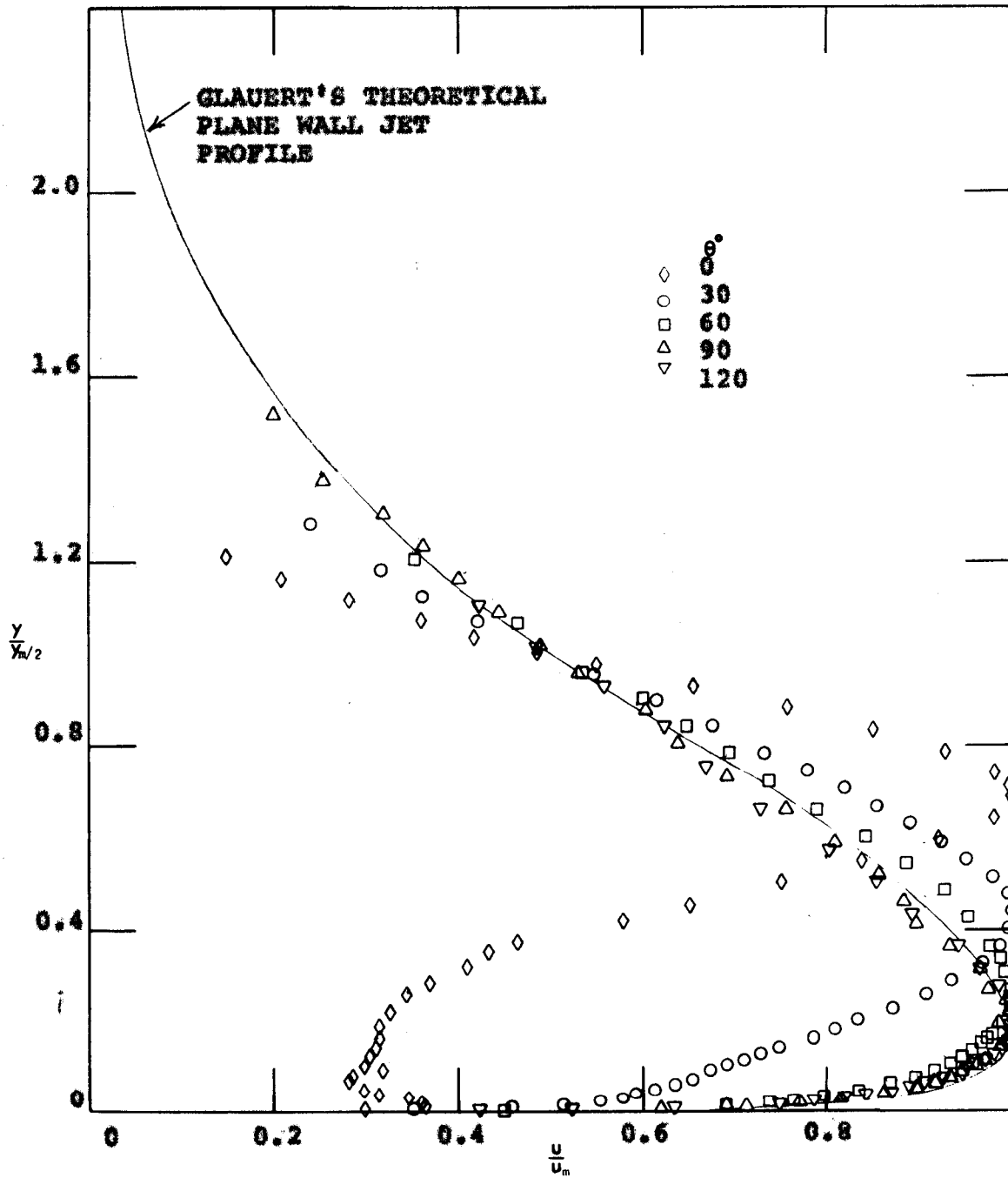


Fig. 13 d. $l' = 12$

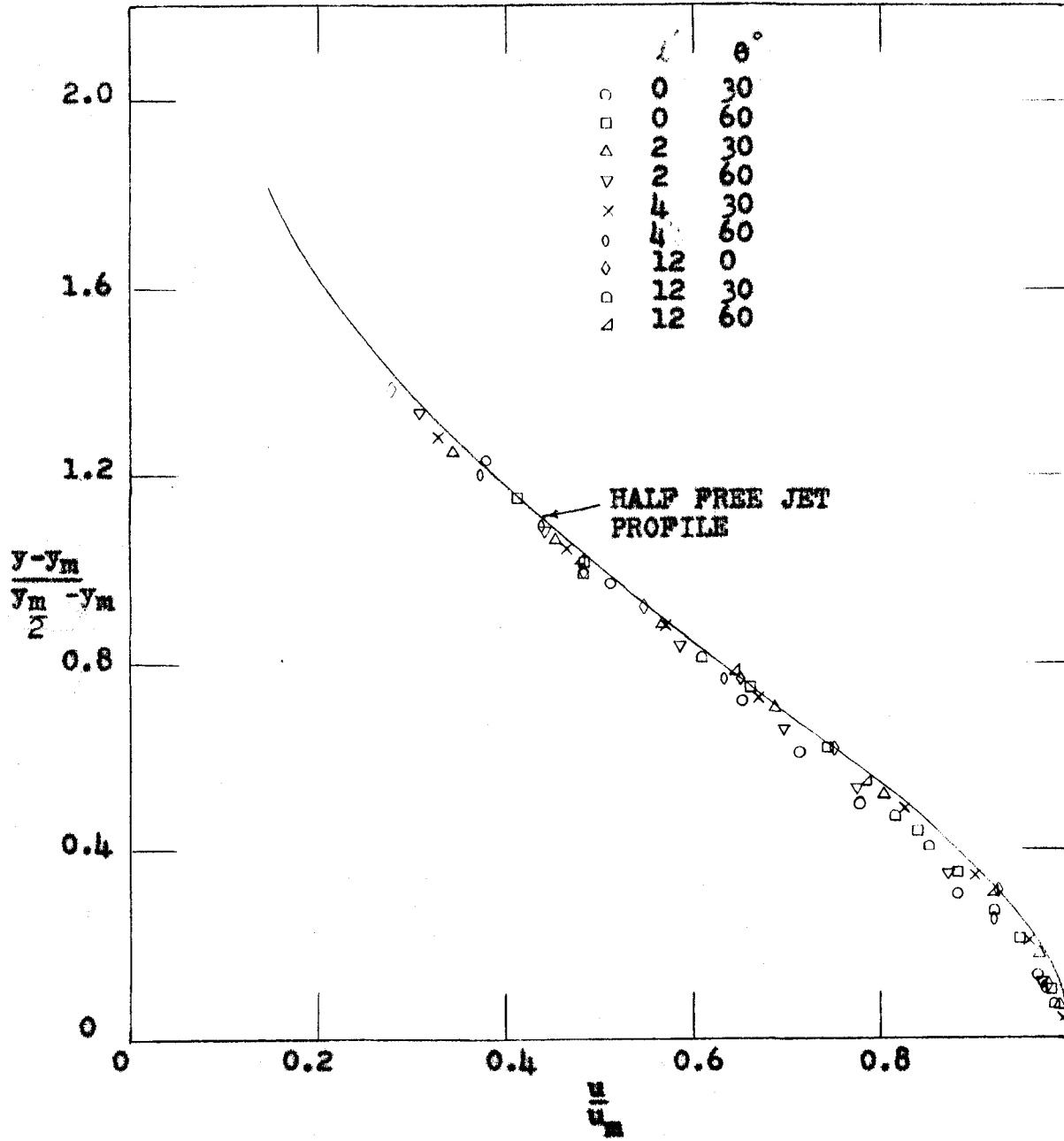


Fig. 14 NON-DIMENSIONAL VELOCITY DISTRIBUTION IN THE OUTER LAYER

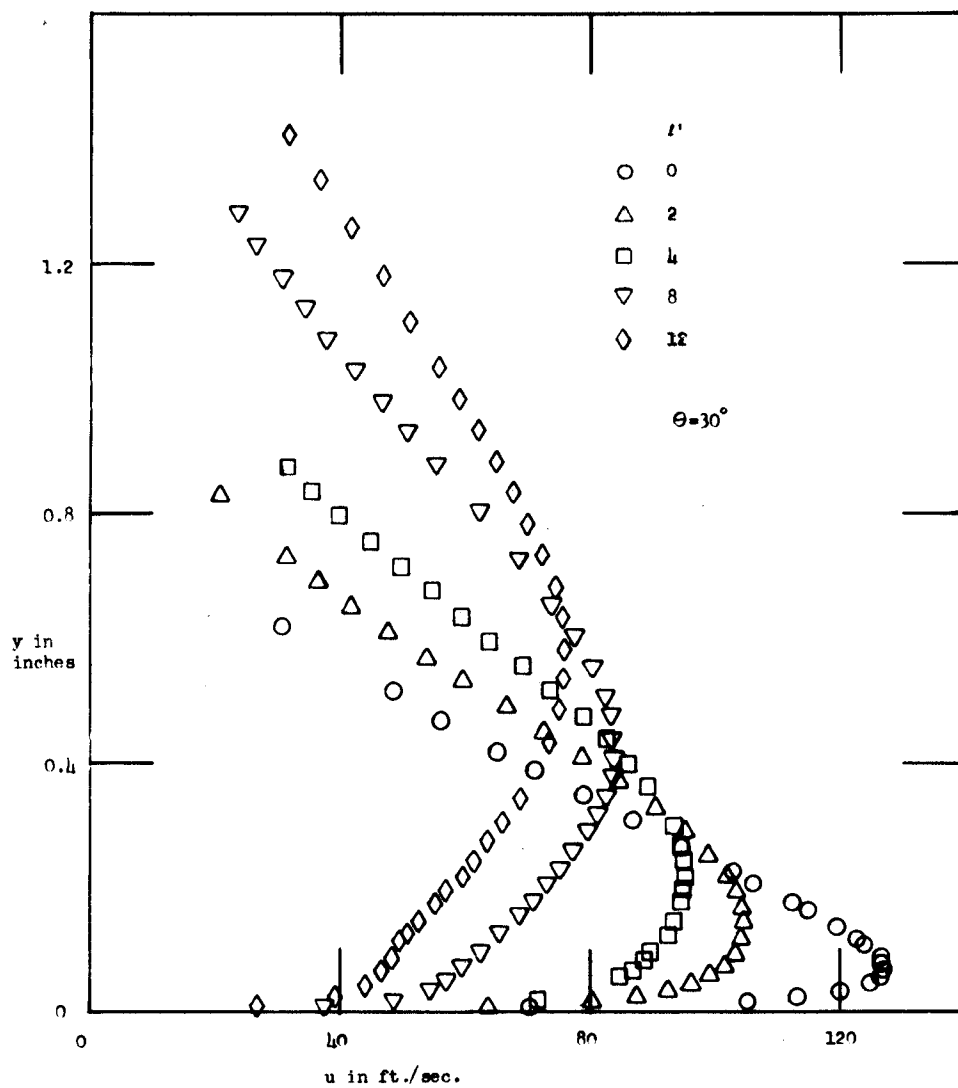


Fig. 15 DIMENSIONAL VELOCITY PROFILES AT $\theta = 30^\circ$
FOR THE GAPS ALONG THE JET BOUNDARY

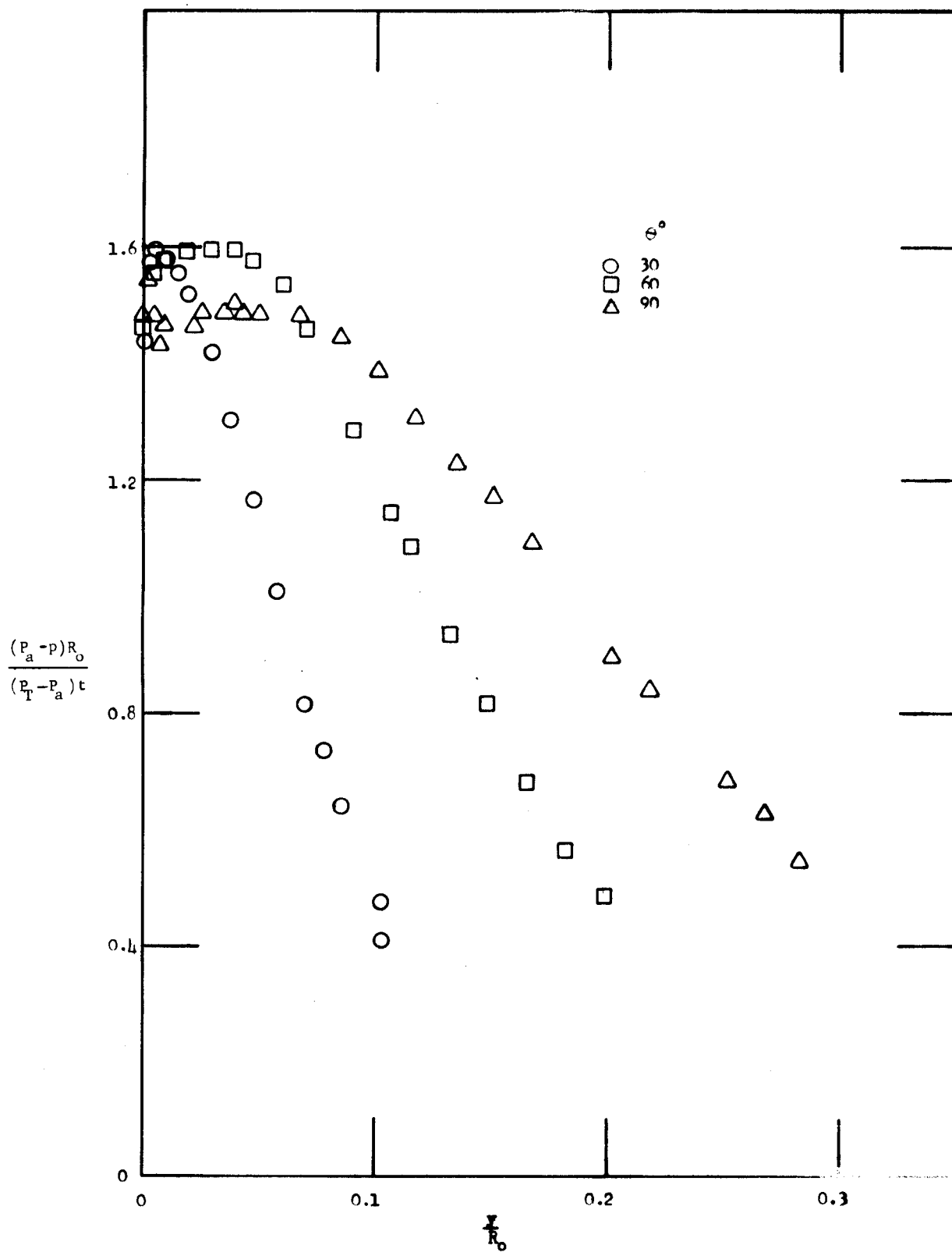


Fig. 16 STATIC PRESSURE DISTRIBUTIONS IN THE JET FOR NO GAP

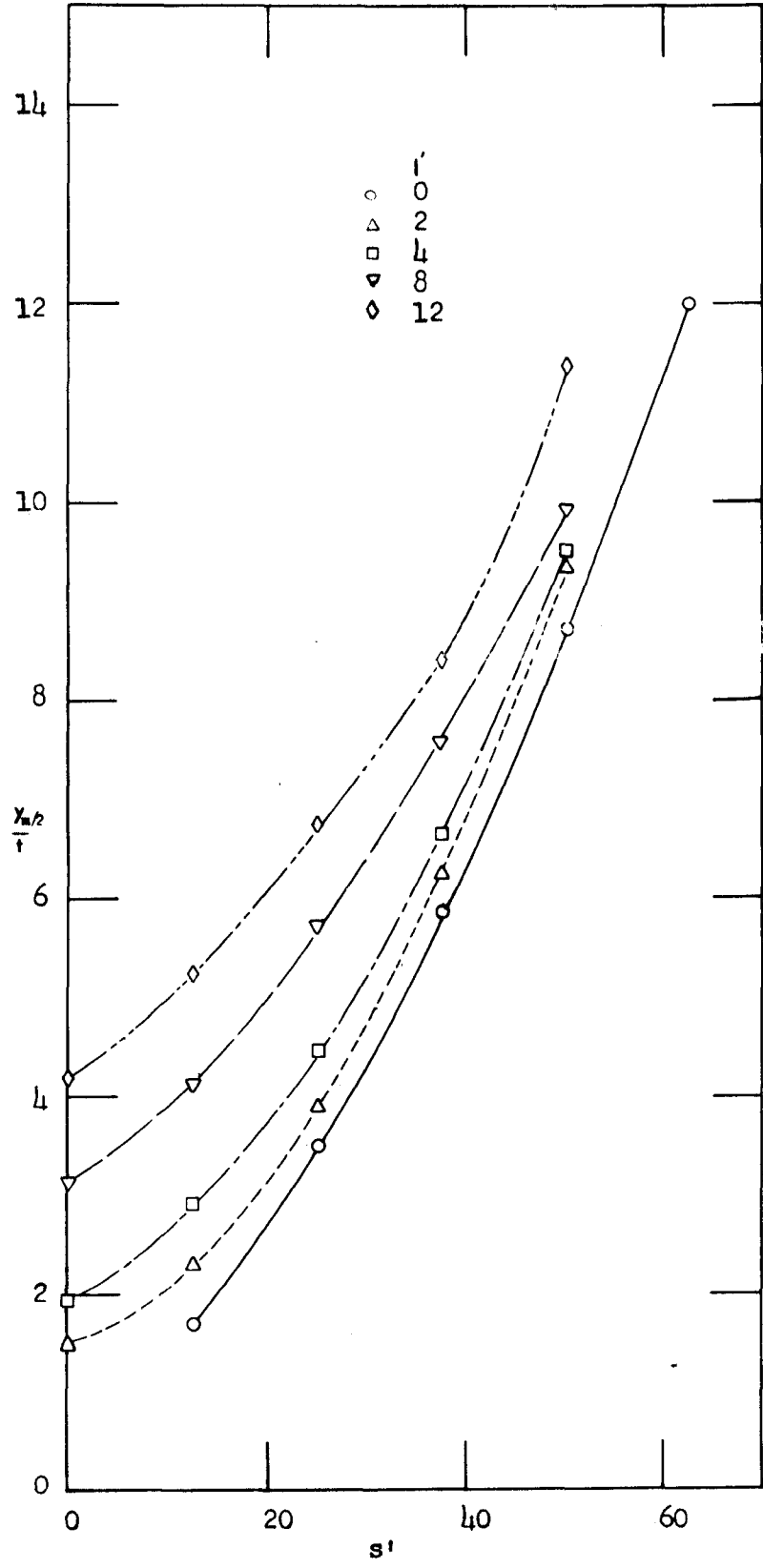


Fig. 17 GROWTH OF CURVED WALL JET FOR GAPS ALONG JET BOUNDARY

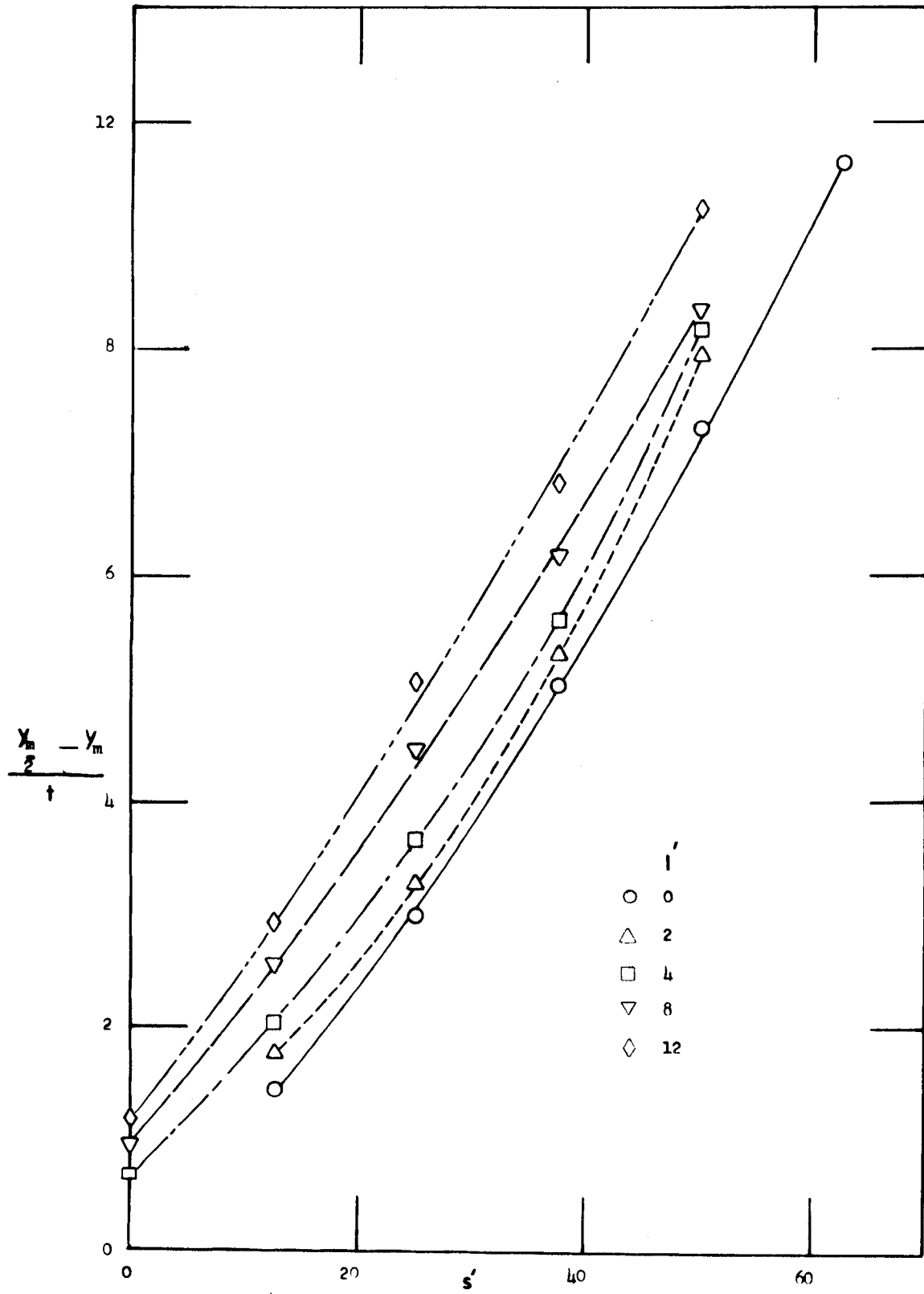


Fig. 18 OUTER LAYER GROWTH FOR GAPS ALONG JET BOUNDARY

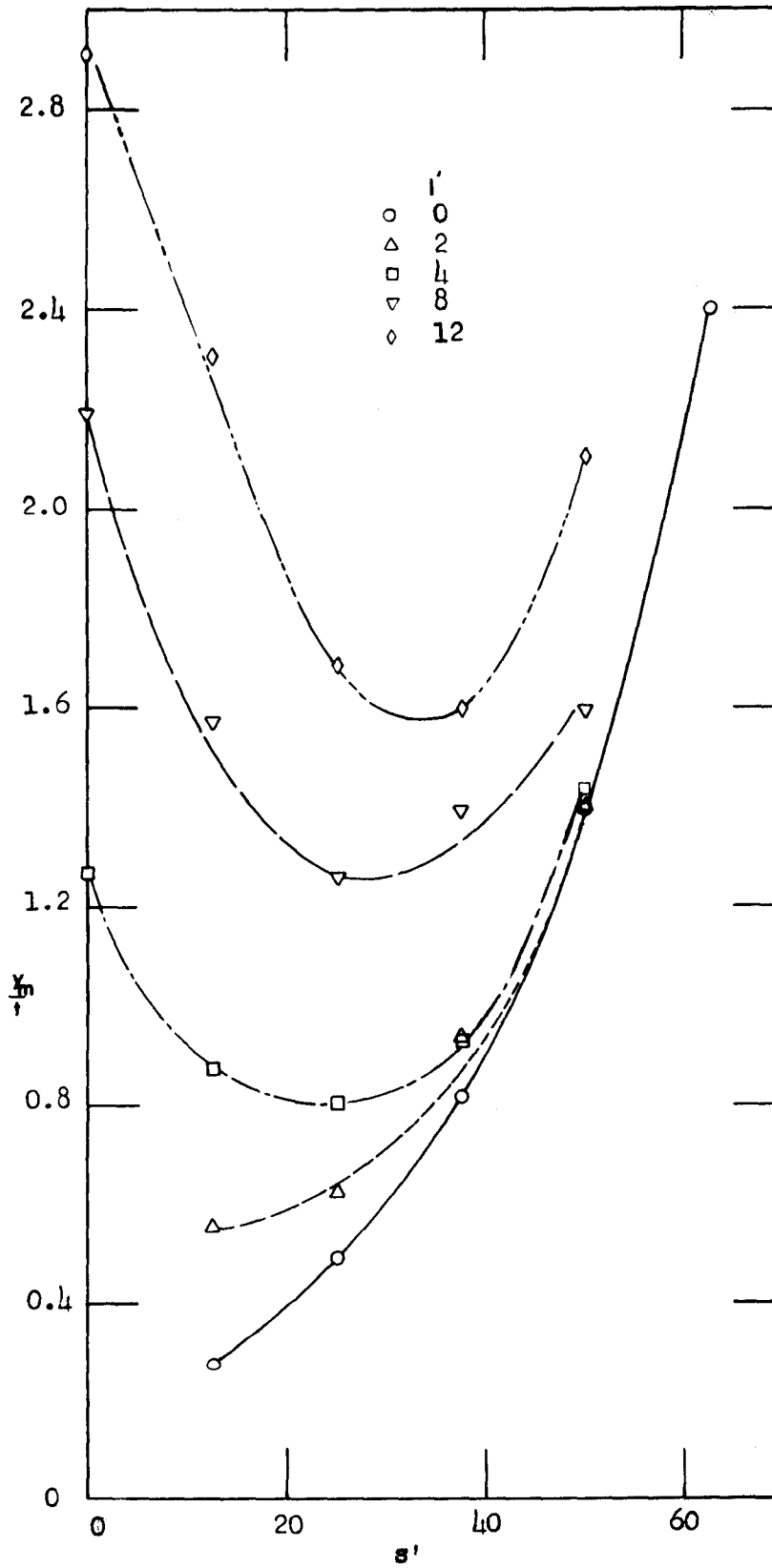


Fig. 19 INNER LAYER GROWTH FOR GAPS ALONG JET BOUNDARY

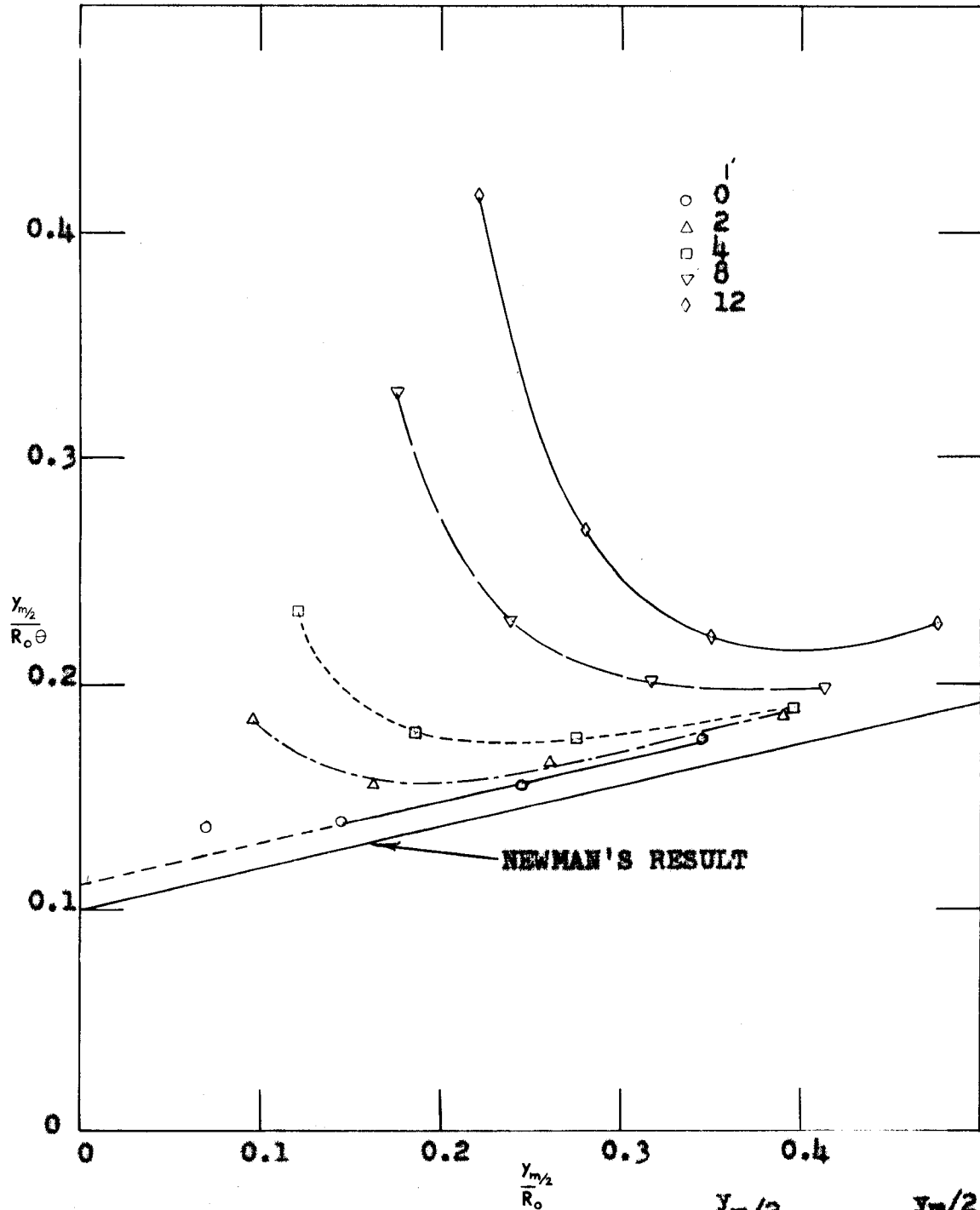


Fig. 20 STREAMWISE VARIATION OF $\frac{y_{m/2}}{R_0 \theta}$ WITH $\frac{y_{m/2}}{R_0}$
FOR THE GAPS ON JET BOUNDARY

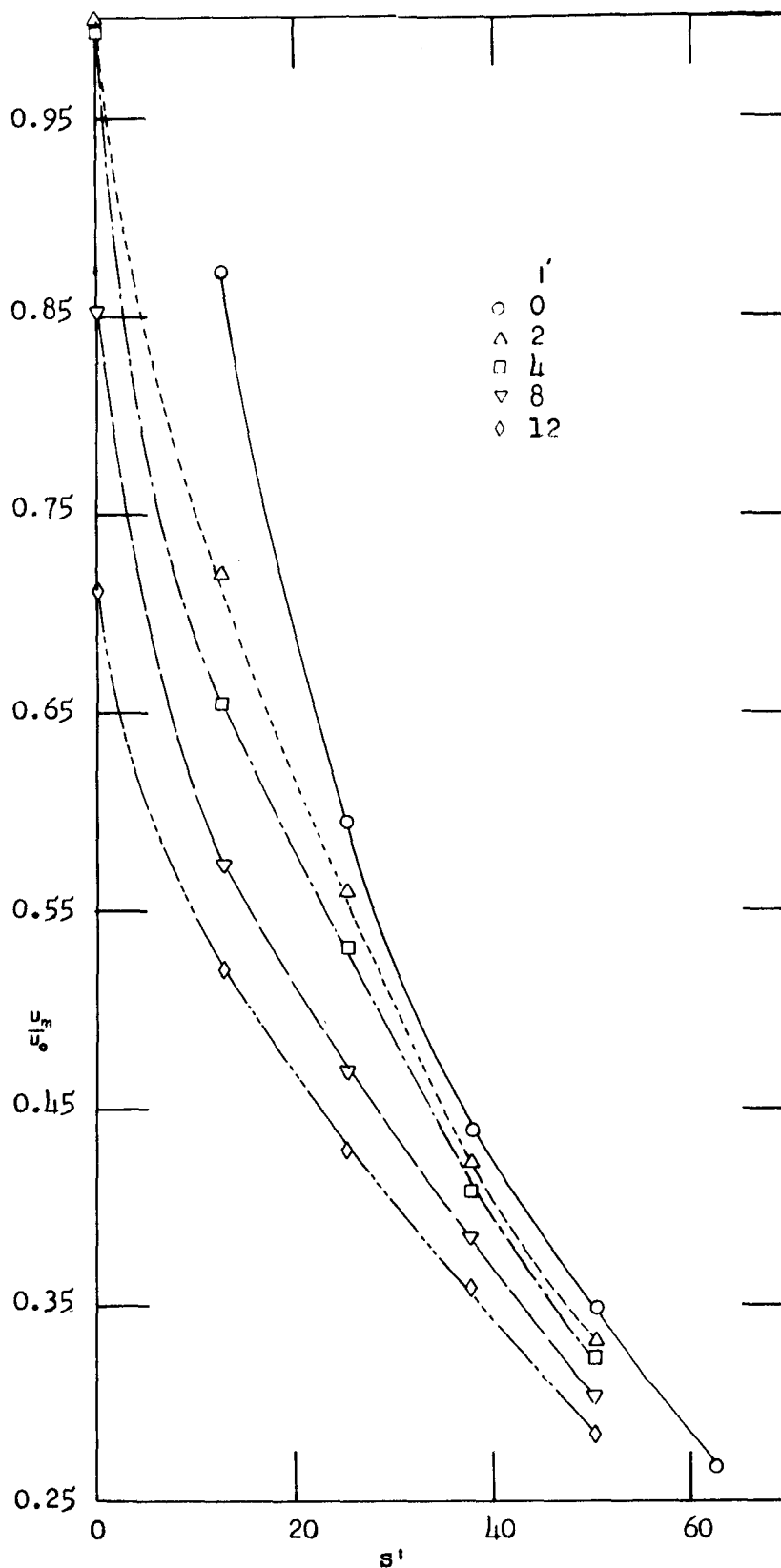


Fig. 21 MAXIMUM VELOCITY DECAY OF CURVED WALL JET WITH GAPS ALONG JET BOUNDARY

UNIVERSITY OF WINDSOR LIBRARY

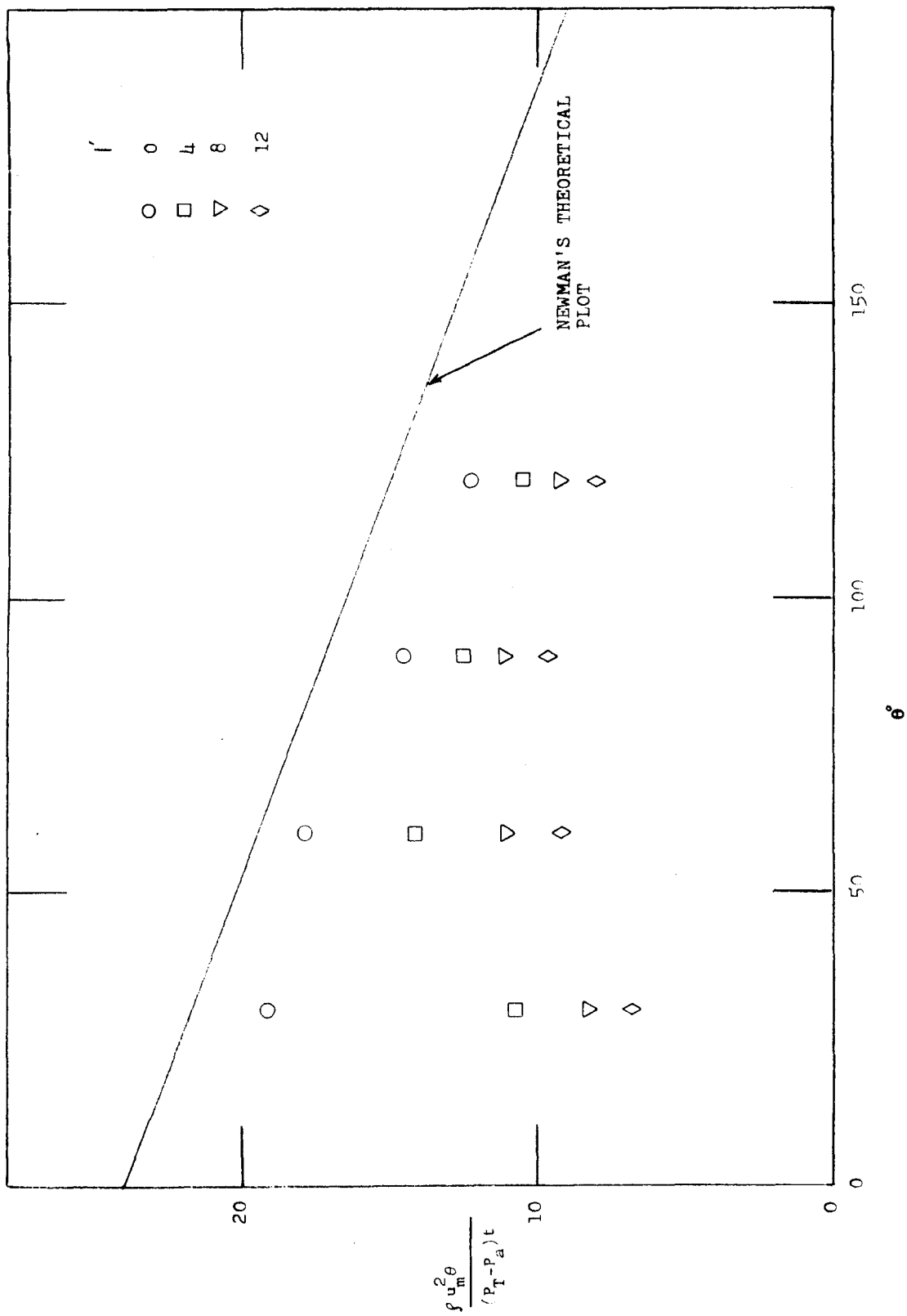


Fig. 22 MAXIMUM VELOCITY DECAY PLOTS (NEWMAN'S METHOD)

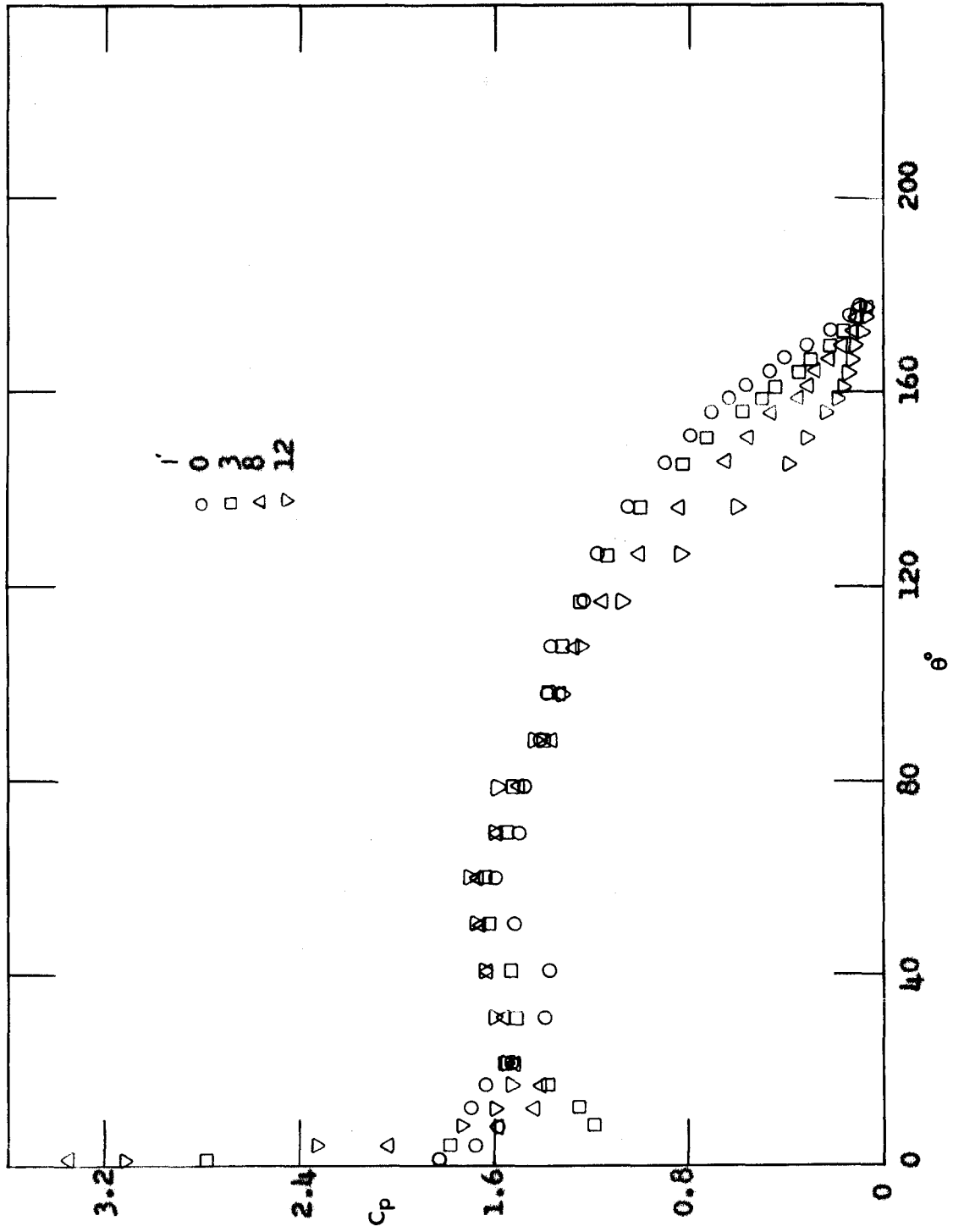


FIG. 23 SURFACE PRESSURE DISTRIBUTIONS

a. FOR GAPS ALONG JET BOUNDARY

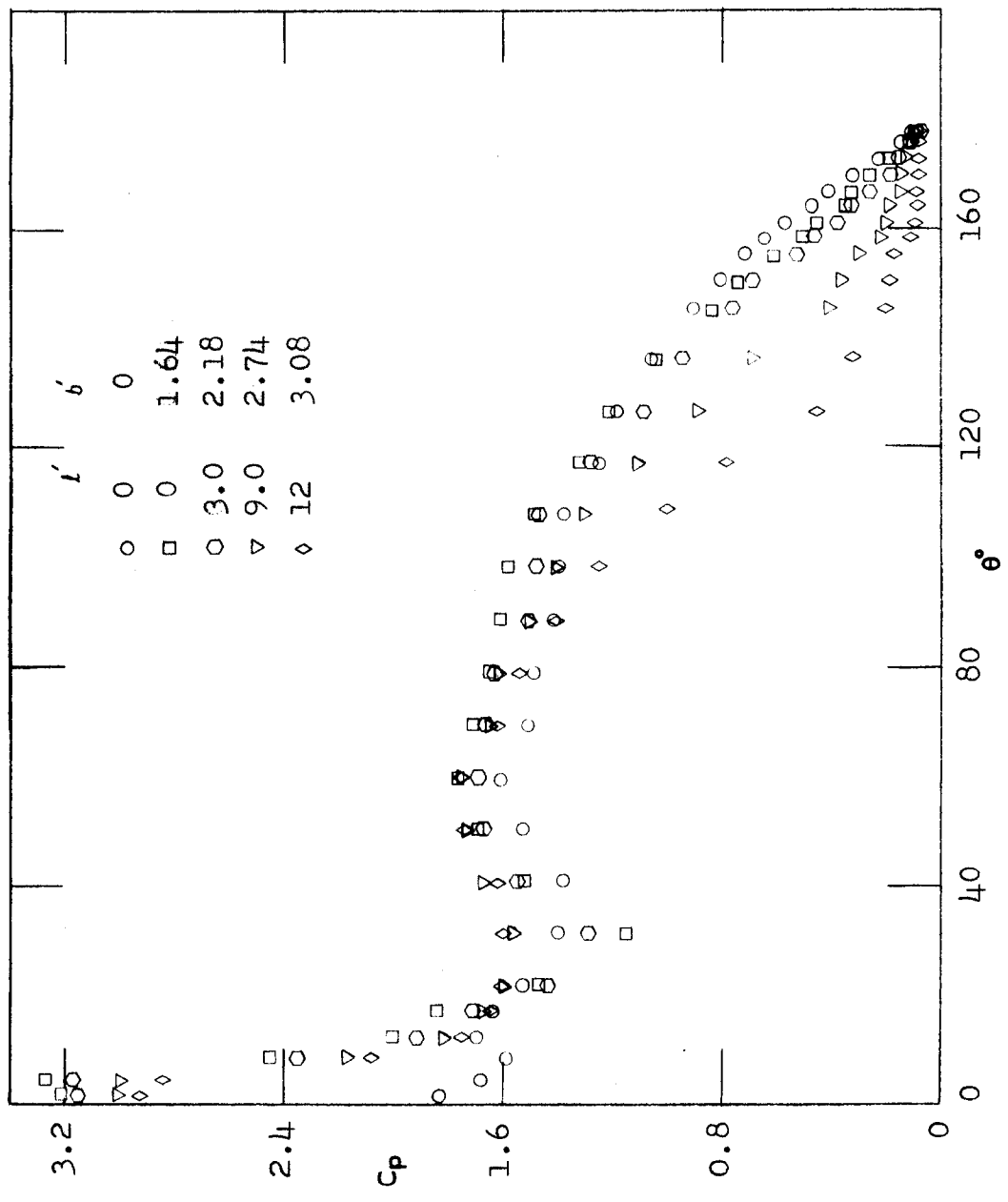
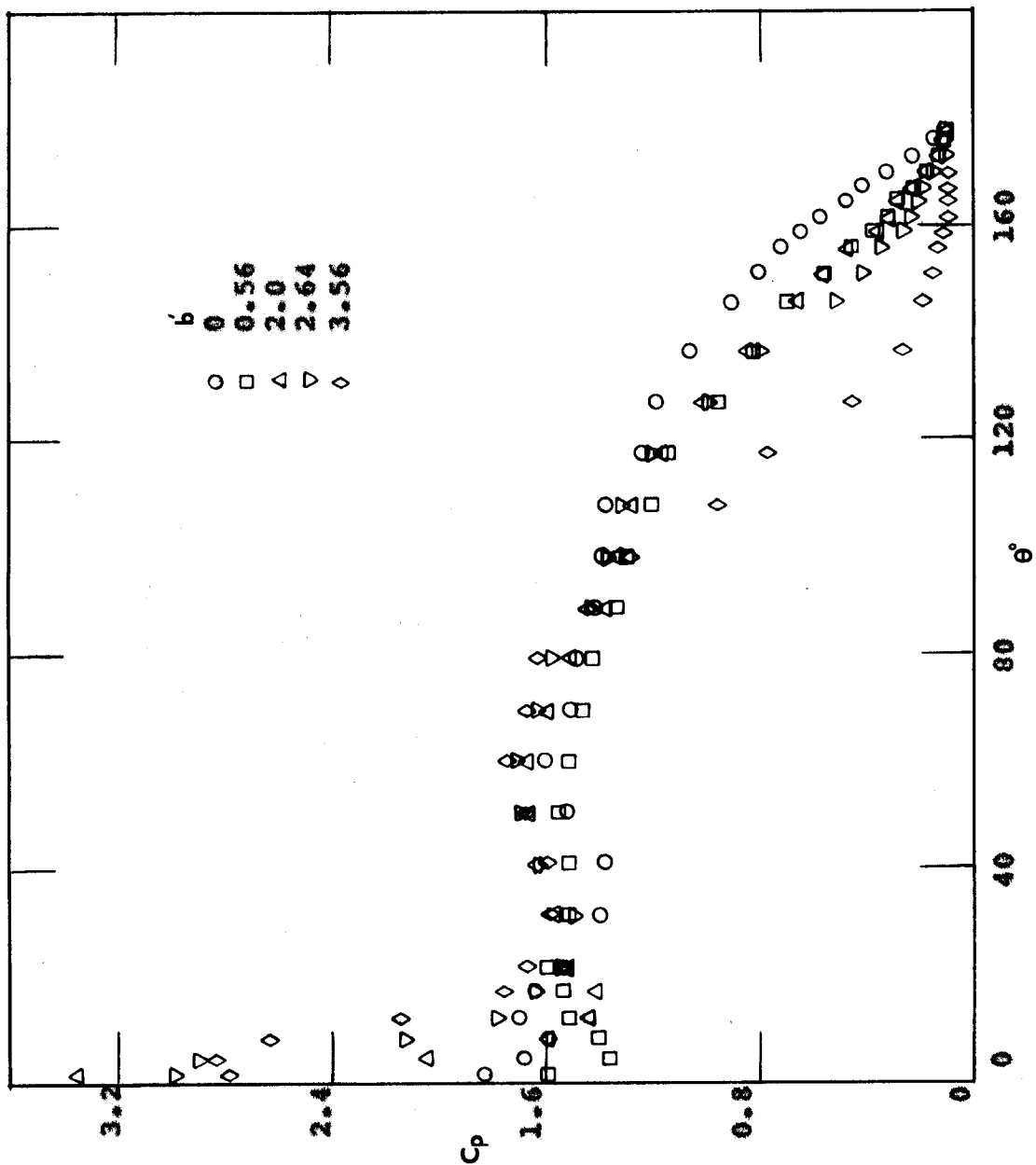


Fig. 23 b. FOR GAPS ALONG "ATTACHED" LINE


 FIG. 23 c. FOR GAPS ALONG LINE DEFINED BY $1^\circ = 8$

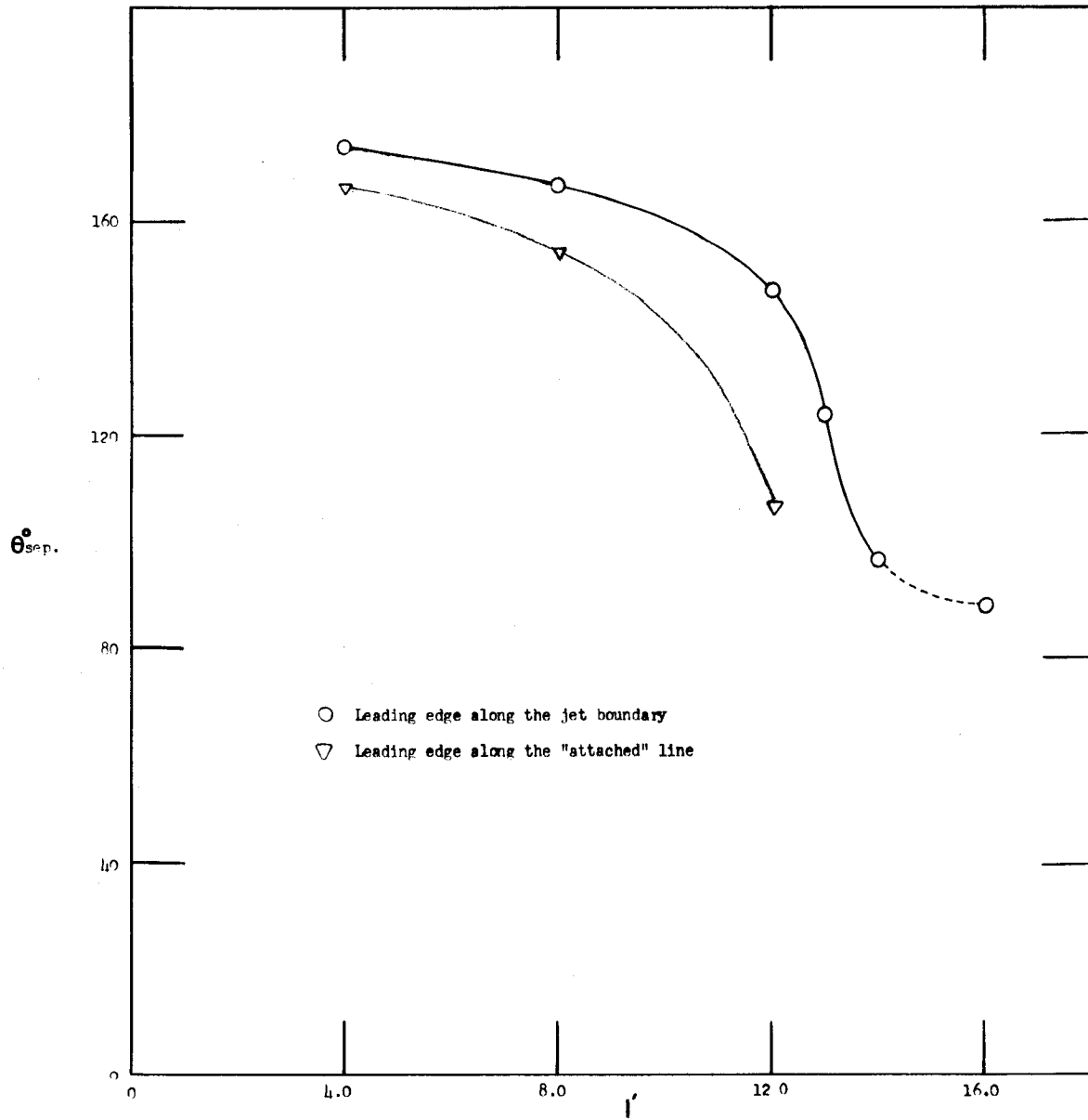


Fig. 24 ANGLE OF SEPARATION FOR THE GAPS ALONG THE JET BOUNDARY AND "ATTACHED" LINE

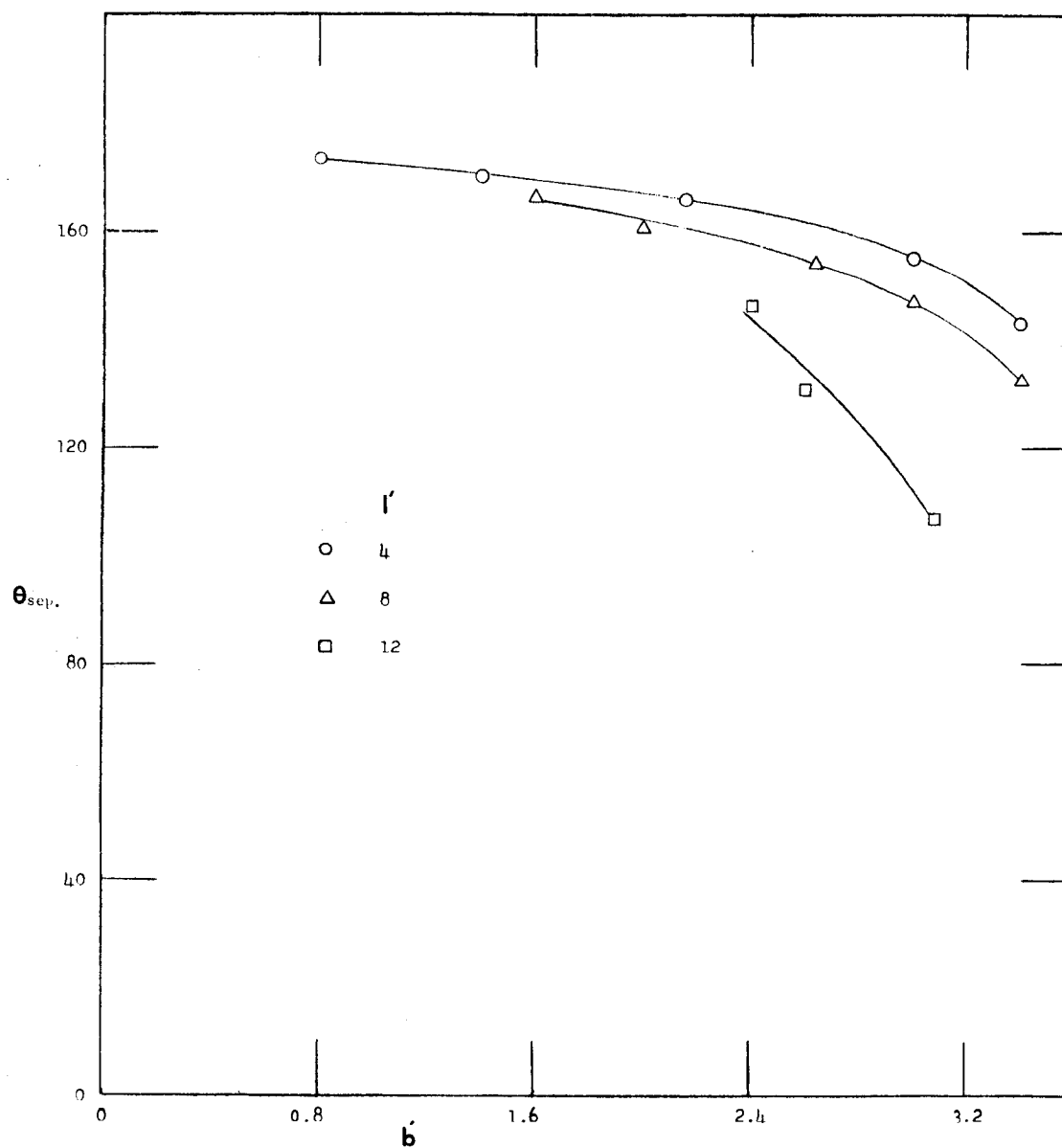


Fig. 25 PLOTS OF $\theta_{sep.}$ VS b FOR DIFFERENT l'

TABLE I
CONSTANTS IN EQUATION 2.8

	Investigator	Probe	C	C_1	k	$Re = \frac{U_o t}{\nu}$
Plane Wall Jet	Sigalla	Pitot	0.0638	8.33	---	2.34×10^4 to 5.35×10^4
	Myers, Schaver and Eustis	Kiel	0.076	6.5	---	1.86×10^4 to 3.47×10^4
	Schwarz and Cosart	Hot Wire	0.0851	7.2	---	1.35×10^4
			0.0694	15.5	---	2.01×10^4
0.0561			12.9	---	3.00×10^4	
0.0607			8.97	---	4.16×10^4	
Curved Wall Jet	Fekete	Pitot	0.1004	2.93	1.839	0.80×10^4
		Hot Wire	0.0731	7.43	3.185	0.80×10^4
	Newman	Pitot	0.11	---	1.5	1.0×10^4
Present Investigation	Pitot	0.11	---	1.67	1.84×10^4	

VITA AUCTORIS

- 1940 Born in Indore, India on October 7.
- 1956 Completed high school education at the H.D. High School, Sholapur, India.
- 1958 Completed Intermediate Science Course at the Fergusson College, Poona, India.
- 1962 B Received the Degree of Bachelor of Science in Mechanical Engineering from the Birla Institute of Technology, Ranchi, India. Employed in the Crompton Parkinson Ltd., Bombay. Later joined the engineering staff of the Heavy Engineering Corporation Ltd., Ranchi, India.
- 1965 Currently a candidate for the Degree of Master of Applied Science in Mechanical Engineering at the University of Windsor.